

2018 Spring

**“Advanced Physical Metallurgy”
- Bulk Metallic Glasses -**

04.11.2018

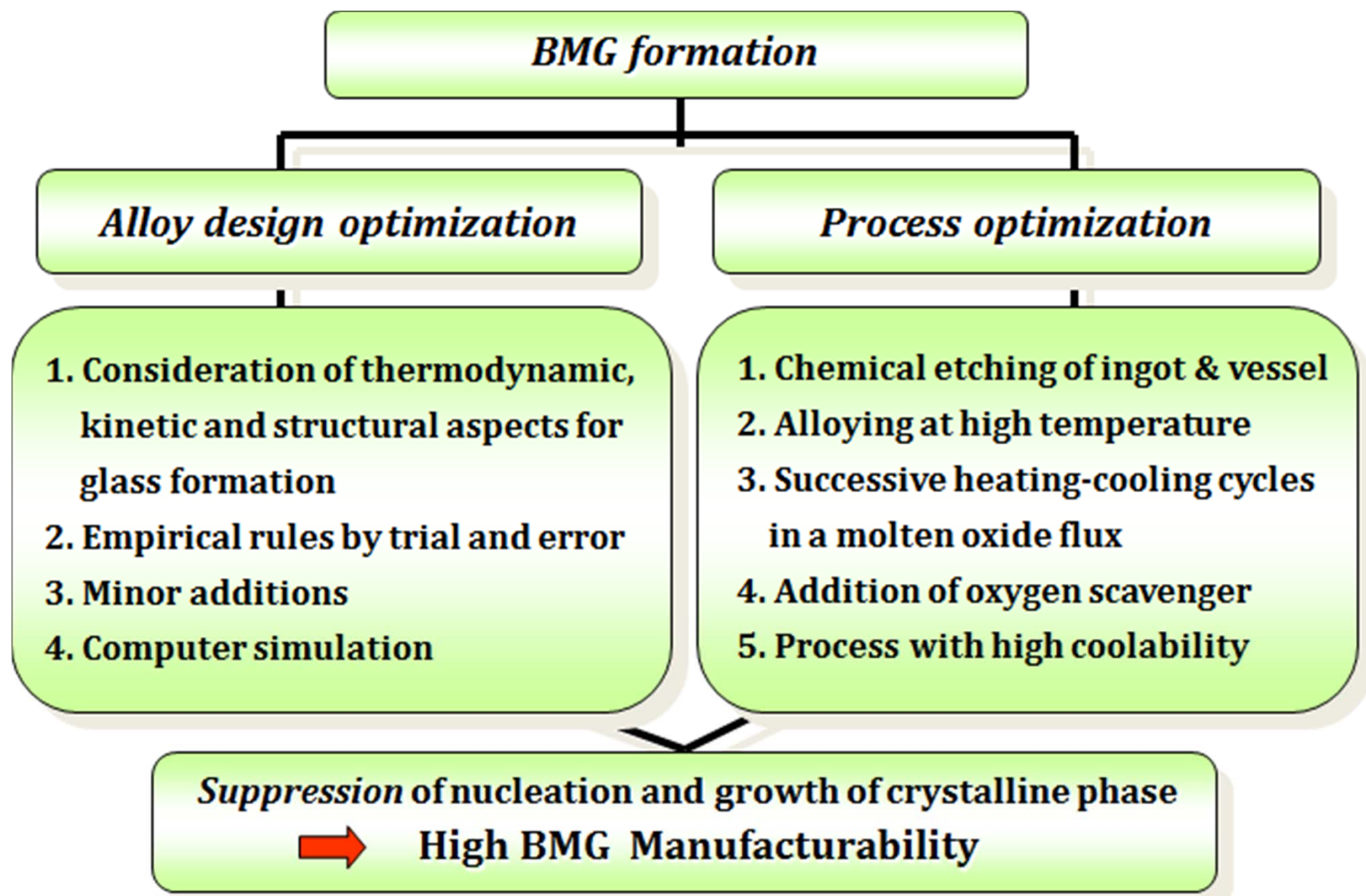
Eun Soo Park

Office: 33-313

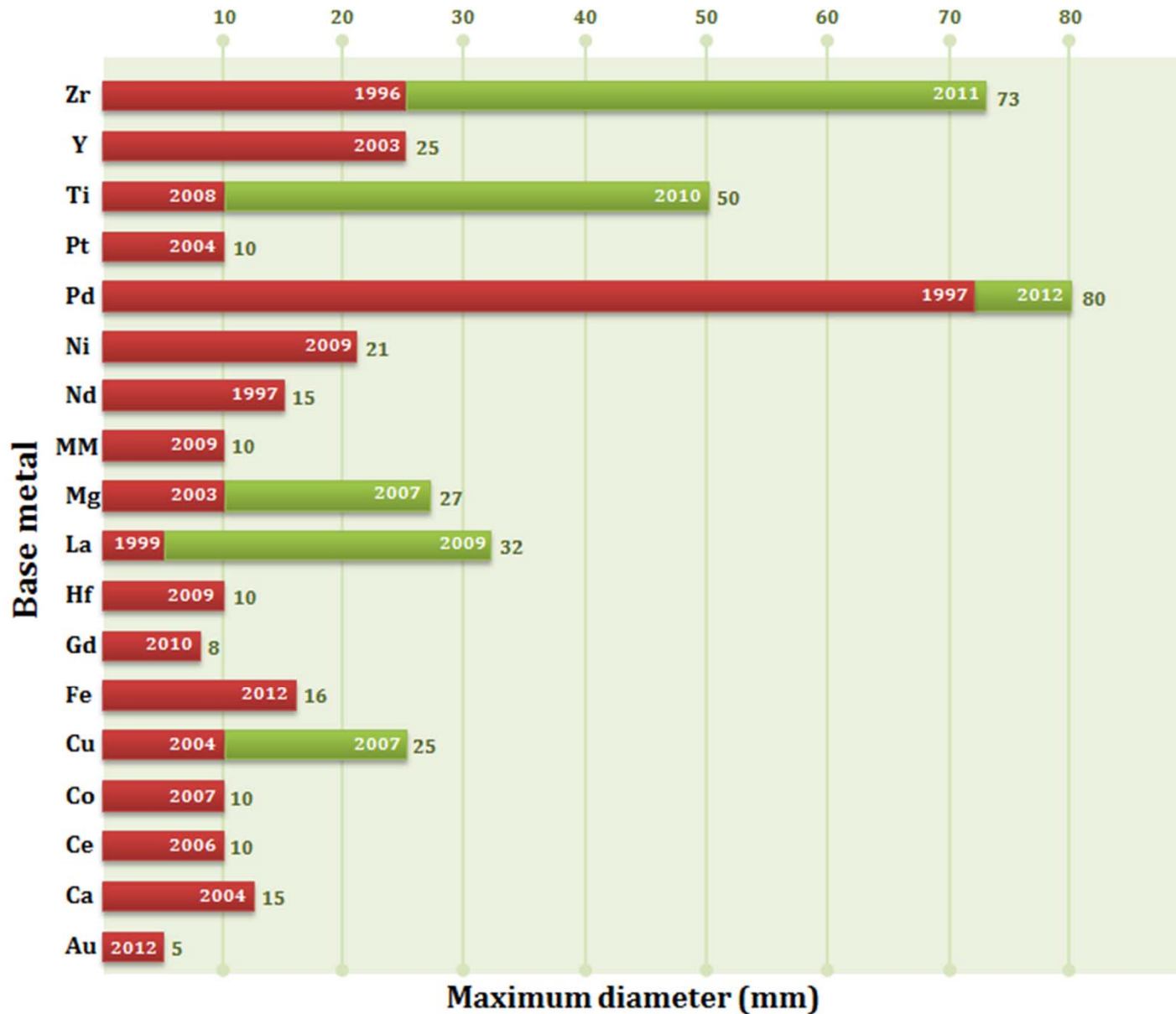
Telephone: 880-7221

Email: espark@snu.ac.kr

Office hours: by appointment



Recent BMGs with critical size ≥ 10 mm



Glass formation

Retention of liquid phase

Formation of crystalline phases

Thermodynamical point

Small change in free E. (liq. → cryst.)

Kinetic point

Low nucleation and growth rates

Structural point

Highly packed random structure

Empirical rules

- (1) multi-component alloy system
- (2) significant difference in atomic size ratios
- (3) negative heats of mixing
- (4) close to a eutectic composition
- (5) compositions far from a Laves phase region

- **Higher degree of dense random packed structure**
- *Suppression* of nucleation and growth of crystalline phase



High glass-forming ability (GFA)

3. Glass-Forming Ability of Alloys

- Many glasses were produced more or less by trial and error.
→ The ability of a metallic alloy to transform into the glassy state is defined in this chapter as the glass-forming ability (GFA).

3.2 Critical Cooling Rate

If an alloy melt is solidified from a temperature above the liquidus temperature, T_l to below the glass transition temperature, T_g , then the volume fraction of the solid crystalline phase, X formed under non-isothermal crystallization conditions can be given by the equation [8,9]

$$X(T) = \frac{4\pi}{3R^4} \int_{T_l}^{T_g} I(T') \left[\int_{T''}^{T_g} U(T'') dT'' \right]^3 dT' \quad (3.1)$$

where I and U are the steady-state nucleation frequency and crystal growth rate,

$$\boxed{X = 10^{-6}} \rightarrow R_c^4 = \frac{4\pi}{3 \times 10^{-6}} \int_{T_l}^{T_g} I(T') \left[\int_{T''}^{T_g} U(T'') dT'' \right]^3 dT' \quad (3.2)$$

Since the equations for I and U contain terms like viscosity of the supercooled liquid, η , entropy of fusion, ΔS_f , etc., the critical cooling rate, R_c decreases with increasing η , ΔS_f , and decreasing liquidus temperature, T_l . The best way to experimentally determine R_c is by constructing the time-temperature-transformation (T - T - T) diagrams.

3.2.1 T-T-T Diagrams: isothermal processes

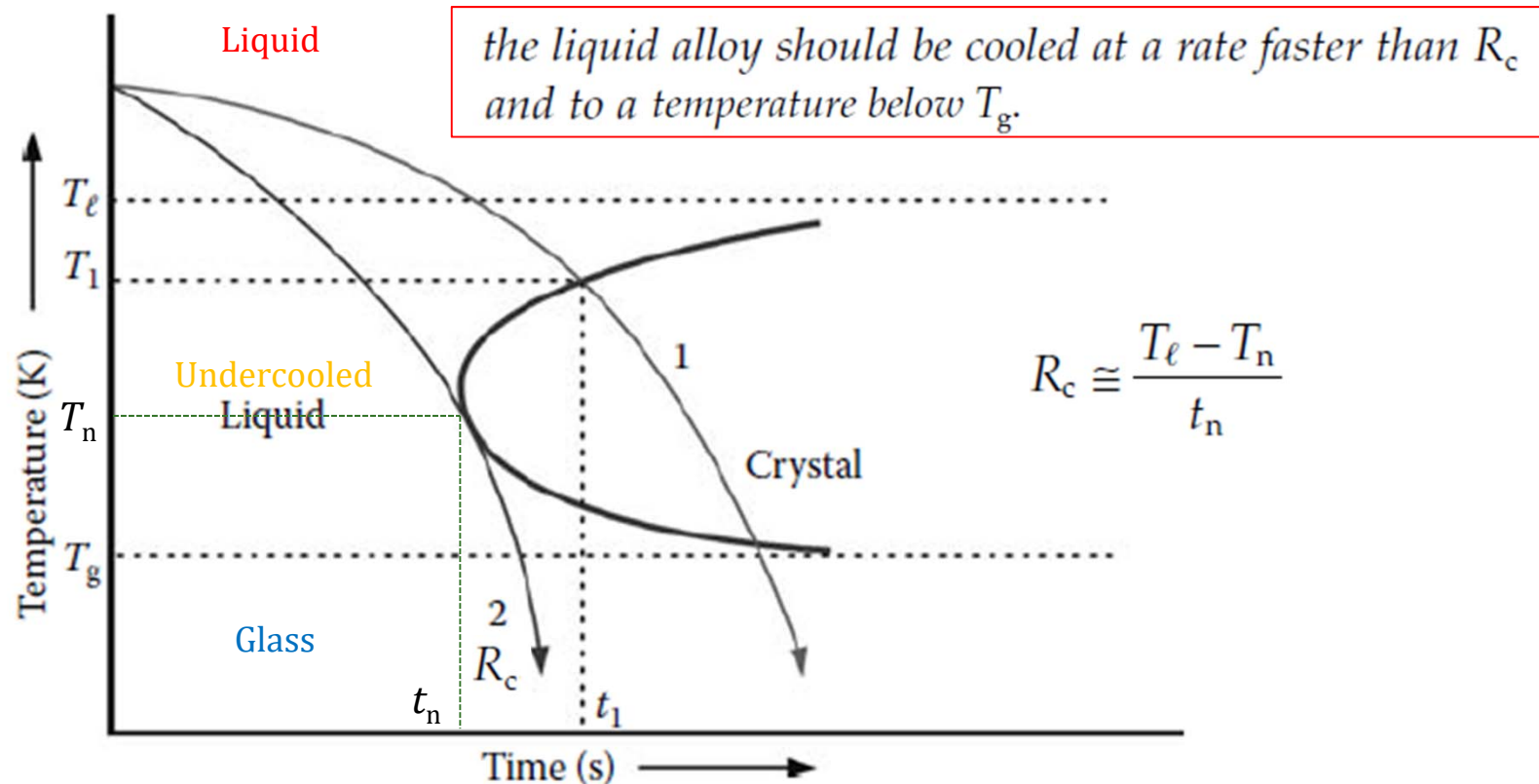


FIGURE 3.1

Schematic time–temperature–transformation (T - T - T) diagram for a hypothetical alloy system. When the liquid alloy is cooled from above the liquidus temperature T_l , at a rate indicated by curve “1,” solidification starts at a temperature T_1 and time t_1 . The resultant product is a crystalline solid. However, if the same liquid alloy is now cooled, again from T_l , at a rate faster than the rate indicated by curve “2,” the liquid will continue to be in the undercooled state, and when cooled below the glass transition temperature T_g , the liquid is “frozen-in” and a glassy phase is formed. The cooling rate represented by curve “2” is referred to as the critical cooling rate, R_c .

R_c vs D_{max} in Ti-Zr-Cu-Ni alloy system

J. Appl. Phys. 78, 1 December 1995

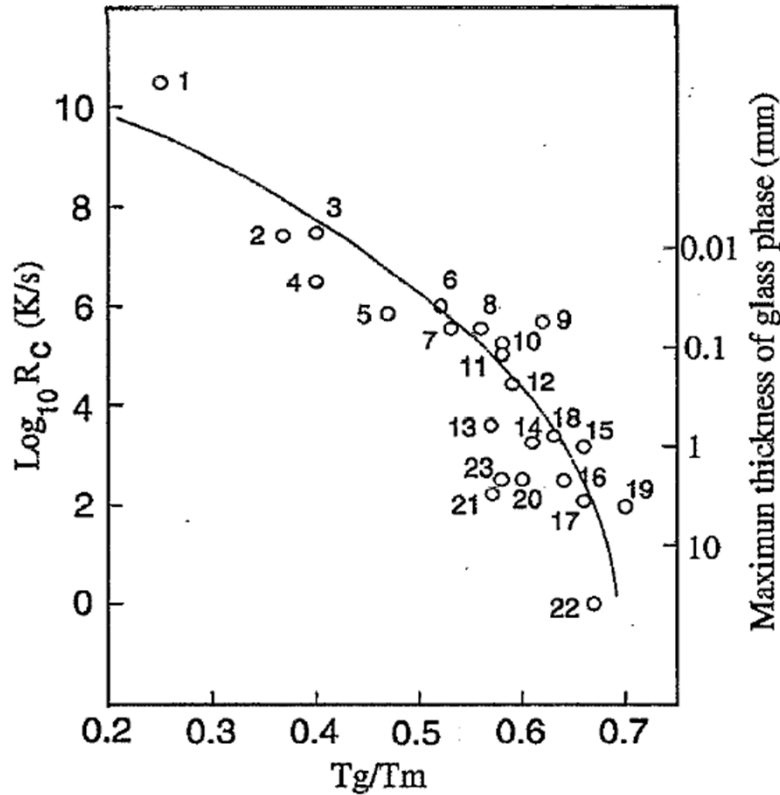


FIG. 1. Critical cooling rates for glass formation and corresponding maximum thickness of glass phase. Key to the alloys: (1) Ni; (2) Fe_{91}B_9 ; (3) $\text{Fe}_{89}\text{B}_{11}$; (4) Te; (5) $\text{Au}_{77.8}\text{Ge}_{13.8}\text{Si}_{8.4}$; (6) $\text{Fe}_{83}\text{B}_{17}$; (7) $\text{Fe}_{41.5}\text{Ni}_{41.5}\text{B}_{17}$; (8) $\text{Co}_{75}\text{Si}_{15}\text{B}_{10}$; (9) Ge; (10) $\text{Fe}_{79}\text{Si}_{10}\text{B}_{11}$; (11) $\text{Ni}_{75}\text{Si}_8\text{B}_{17}$; (12) $\text{Fe}_{80}\text{P}_{13}\text{C}_7$; (13) $\text{Pt}_{60}\text{Ni}_{15}\text{P}_{25}$; (14) $\text{Pd}_{82}\text{Si}_{18}$; (15) $\text{Ni}_{62.4}\text{Nb}_{37.6}$; (16) $\text{Pd}_{77.5}\text{Cu}_6\text{Si}_{16.5}$; (17) $\text{Pd}_{40}\text{Ni}_{40}\text{P}_{20}$ (above from Ref. 3); (18) $\text{Au}_{55}\text{Pb}_{22.5}\text{Sb}_{22.5}$ (Ref. 6); (19) $\text{La}_{55}\text{Al}_{25}\text{Ni}_{10}\text{Cu}_{10}$ (Ref. 7); (20) $\text{Mg}_{65}\text{Cu}_{25}\text{Y}_{10}$ (Ref. 8); (21) $\text{Zr}_{65}\text{Cu}_{17.5}\text{Ni}_{10}\text{Al}_{7.5}$ (Ref. 9); (22) $\text{Zr}_{41.2}\text{Ti}_{13.8}\text{Cu}_{12.5}\text{Ni}_{10}\text{Be}_{22.5}$ (Refs. 4 and 5); (23) $\text{Ti}_{34}\text{Zr}_{11}\text{Cu}_{47}\text{Ni}_8$.

Total cooling time $\tau \sim (R^2/\kappa)$

sample dimension (dia. or thickness) : R

initial temperature: T_m

thermal diffusivity : κ

$$\kappa = K/C$$

thermal conductivity : K

heat capacity per unit volume: C

$$\dot{T} = \frac{dT}{dt} = \frac{(T_m - T_g)}{\tau} = \frac{K(T_m - T_g)}{CR^2}$$

For Ti-Zr-Cu-Ni system,

$$T_m - T_g \sim 400\text{K} \quad K \sim 0.1\text{W/cm s}^{-1}\text{K}^{-1} \quad C \sim 4\text{J/cm}^3\text{K}^{-1}$$

$$\dot{T} \text{ (K/s)} = 10/R^2 \text{ (cm)}$$

3.2.2. Effect of Alloying Elements

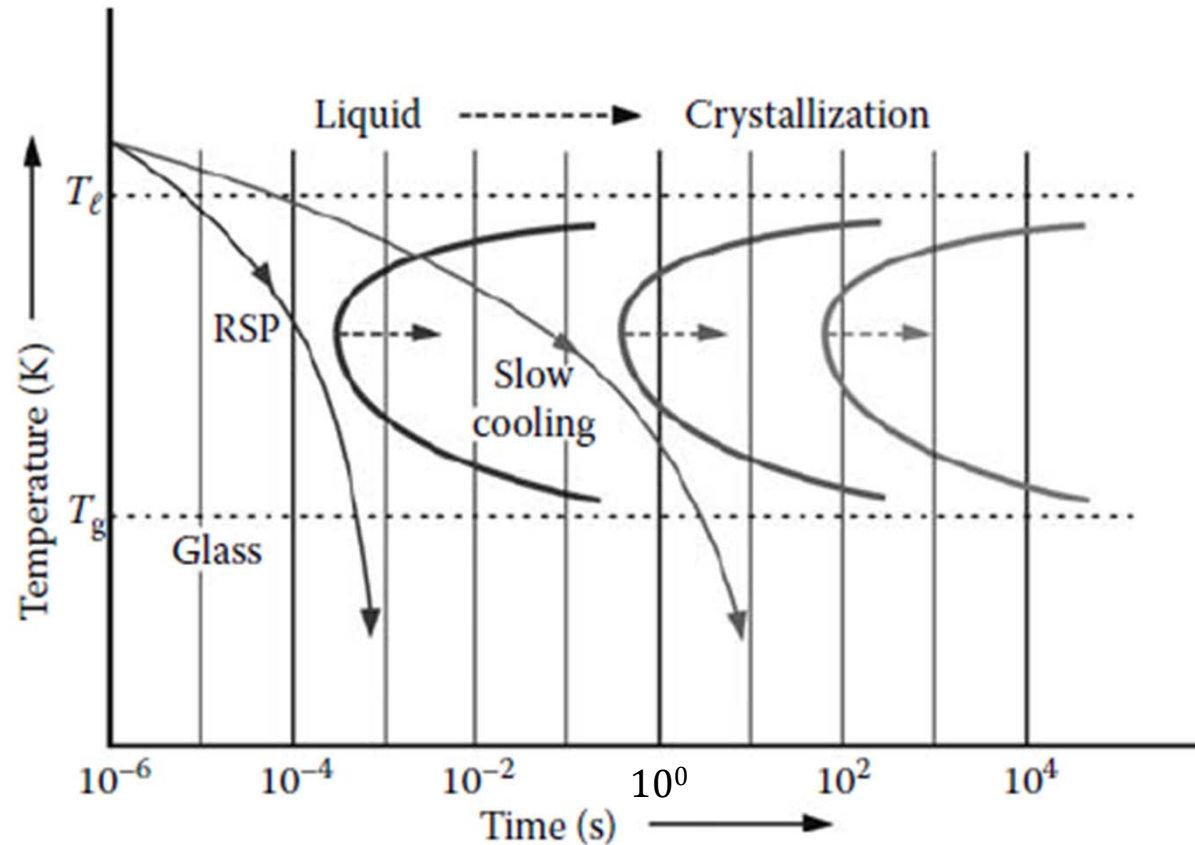


FIGURE 3.2

Position of the T - T - T curves with the addition of a large number of alloying elements. The C-curve shifts to the right with increasing number of alloying elements and consequently, the glassy phase can be synthesized at slow solidification rates. The left-most C-curve represents a typical situation of an alloy system where a glassy phase is obtained by rapid solidification processing (RSP) from the liquid state. The middle C-curve represents an alloy composition where a glassy phase can be obtained by slow cooling. The right-most C-curve represents a situation when an alloy can be very easily produced in a glassy state.

R_c

$> 10^{10-12}$ K/s 10^{4-6} K/s 10^2 K/s 1.3×10^{-2} or 0.067 K/s 10^{-5} to 10^{-4} K/s
 pure metals binary typically $\text{Pd}_{37.5}\text{Cu}_{32.5}\text{Ni}_{10}\text{P}_{20}$ Oxide glasses
 metallic liquids, multicomponent $\text{Pd}_{30}\text{Pt}_{17.5}\text{Cu}_{32.5}\text{P}_{20}$

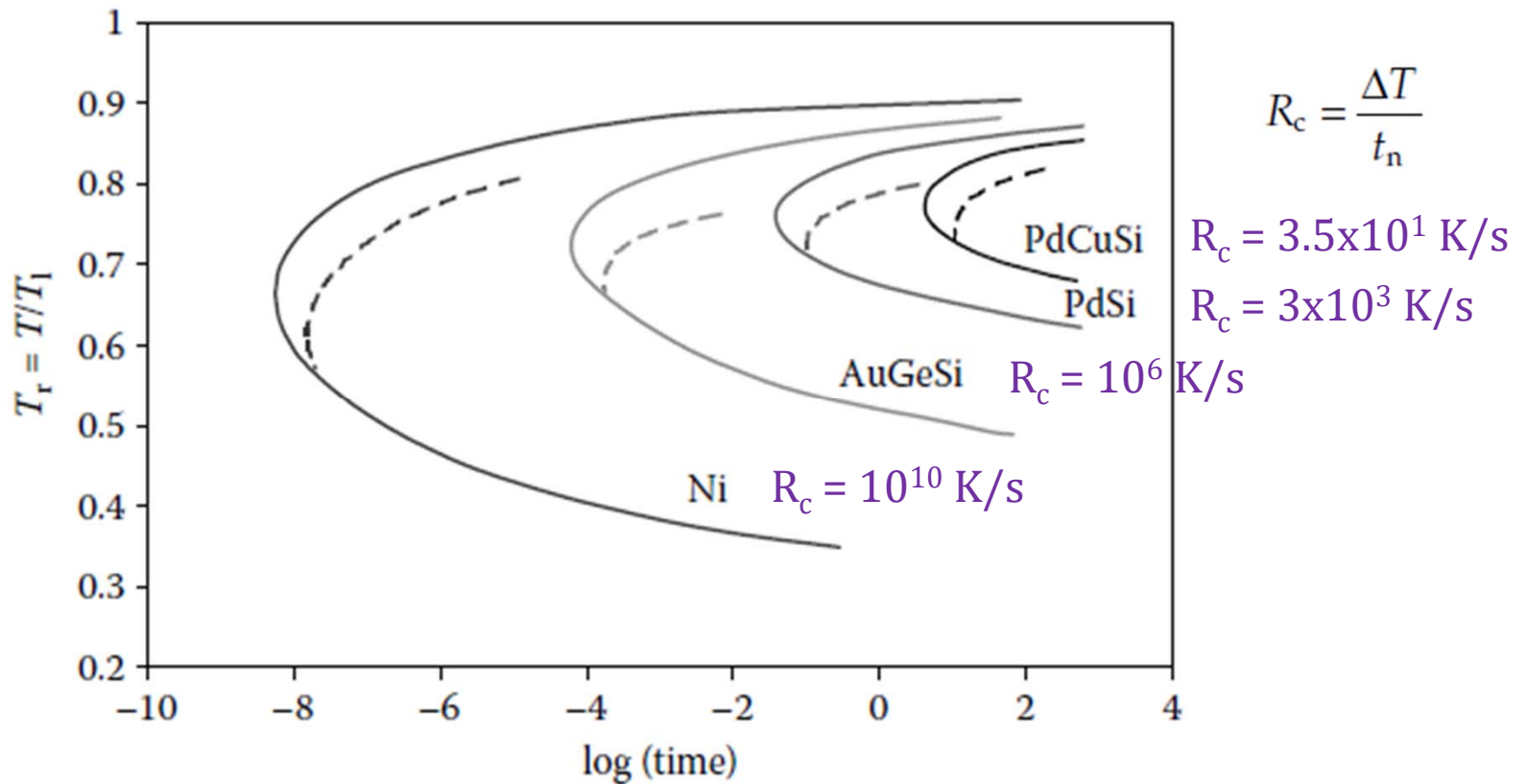


FIGURE 2.3

Time-temperature-transformation (T - T - T) curves (solid lines) and the corresponding continuous cooling transformation curves (dashed lines) for the formation of a small volume fraction for pure metal Ni, and $\text{Au}_{78}\text{Ge}_{14}\text{Si}_8$, $\text{Pd}_{82}\text{Si}_{18}$, and $\text{Pd}_{78}\text{Cu}_6\text{Si}_{16}$ alloys.

T_{rg}

Ni

1/4

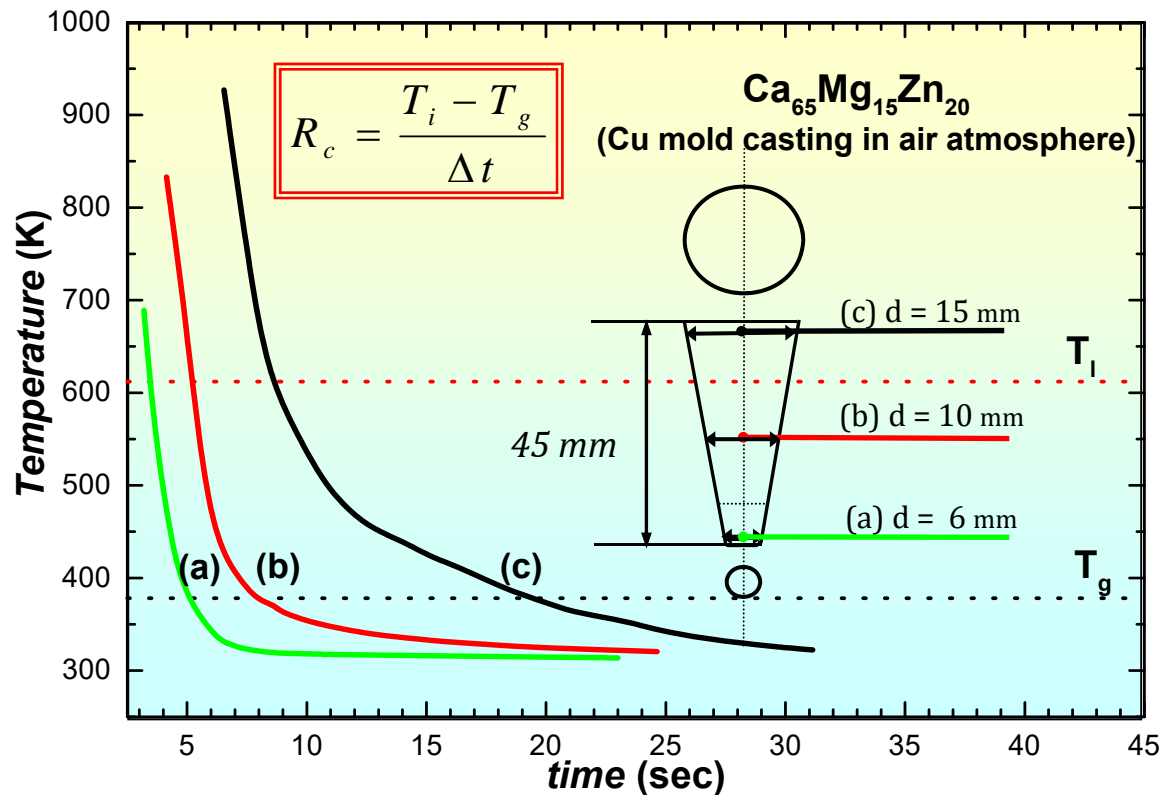
1/2

2/3

3.2.3 Measurement of R_c

The measurement of R_c is an involved and time-consuming process. One has to take a liquid alloy of a chosen composition and allow it to solidify at different cooling rates and determine the nature and amount of phases formed after solidification.

Measurement of R_c in $\text{Ca}_{65}\text{Mg}_{15}\text{Zn}_{20}$ ($D_{\text{max}} > 15 \text{ mm}$)



top position : 20 K/s

middle position : 93 K/s

bottom position : 149 K/s

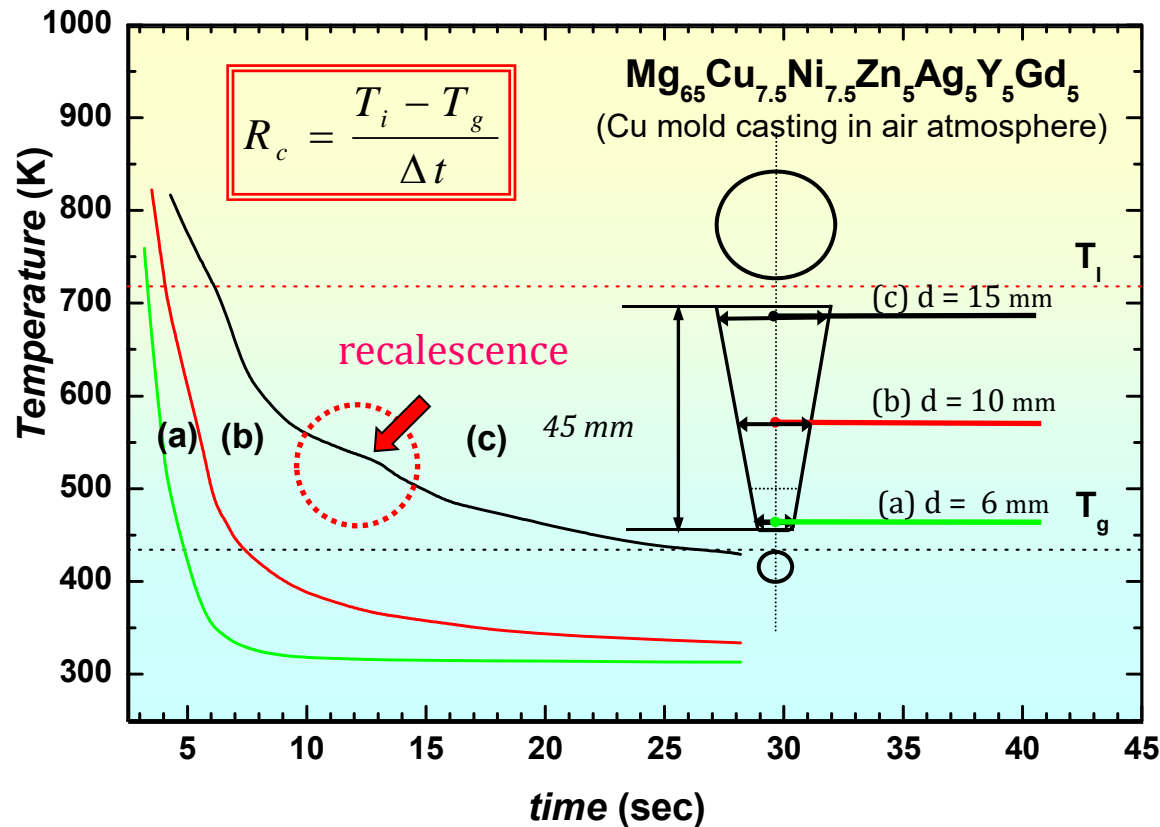
* Cooling curves measured at the center of the three transverse cross sections

* J. Mater. Res. 19, 685 (2004)

* Mater. Sci. Forum 475-479, 3415 (2005)

3.2.3 Measurement of R_c

Measurement of R_c in Mg BMG ($D_{\max}=14$ mm)



top position : recalescence

middle position : 64K/s

bottom position : 137 K/s

* Cooling curves measured at the center of the three transverse cross sections

* JAP 104, 023520 (2008)

TABLE 3.1

Some Representative Critical Cooling Rates (R_c) for Formation of Glassy Phases in Different Alloy Systems

1) Effect of B_2O_3 fluxing

$Pd_{40}Cu_{30}Ni_{10}P_{20}$ $1.58 K s^{-1}$ without fluxing [22]
 $0.1 K s^{-1}$ with fluxing [18]

2) Effect of # of components

$Pd_{82}Si_{18}$ $1.8 \times 10^3 K s^{-1}$ \longleftrightarrow $550 K s^{-1}$ $Pd_{78}Cu_6Si_{16}$
 $Cu_{50}Zr_{50}$ $250 K s^{-1}$ \longleftrightarrow $\leq 40 K s^{-1}$ $Cu_{48}Zr_{48}Al_4$

3) Nature of alloying addition

$Mg_{65}Cu_{25}Y_{10}$ $100 K s^{-1}$ \longleftrightarrow $Mg_{65}Cu_{25}Gd_{10}$ $1 K s^{-1}$ \longleftrightarrow $Mg_{65}Cu_{15}Ag_5Pd_5Gd_{10}$ $0.7 K s^{-1}$

Alloy Composition	R_c ($K s^{-1}$)	Reference
$Au_{77.8}Ge_{13.8}Si_{8.4}$	3×10^6	[24]
$Ca_{60}Mg_{25}Ni_{15}$	24	[25]
$Ca_{65}Mg_{15}Zn_{20}$	<20	[26]
$Cu_{50}Zr_{50}$	250	[27]
$Cu_{48}Zr_{48}Al_4$	<40	[27]
$Cu_{42}Zr_{42}Ag_8Al_8$	4.4	[28]
$Fe_{43}Cr_{16}Mo_{16}C_{10}B_5P_{10}$	100	[29]
$Fe_{40}Ni_{40}P_{14}B_6$ (Metglas 2826)	4.4×10^7	[30]
$Hf_{70}Pd_{20}Ni_{10}$	124	[31]
$La_{55}Al_{25}Cu_{20}$	58	[32]
$La_{55}Al_{25}Ni_{20}$	69	[32]
$Mg_{65}Cu_{25}Gd_{10}$	1	[16]
$Mg_{65}Cu_{25}Y_{10}$	100	[33]
$Mg_{65}Cu_{15}Ag_5Pd_5Gd_{10}$	0.7	[34]
$Mg_{65}Cu_{7.5}Ni_{7.5}Ag_5Zn_5Gd_5Y_5$	20	[35]
$Nd_{60}Co_{30}Al_{10}$	4	[36]
$Ni_{62}Nb_{38}$	57	[37]
$Ni_{65}Pd_{15}P_{20}$	10^5	[38]
$Pd_{78}Cu_6Si_{16}$	550	[39]
$Pd_{40}Ni_{40}P_{20}$	128	[22]
$Pd_{42.5}Cu_{30}Ni_{7.5}P_{20}$	0.067	[18]
$Pd_{40}Cu_{25}Ni_{15}P_{20}$	0.150	[18]
$Pd_{40}Cu_{30}Ni_{10}P_{20}$ (without fluxing)	1.58	[22]
$Pd_{40}Cu_{30}Ni_{10}P_{20}$ (with flux treatment)	0.1	[18]
$Pd_{30}Pt_{17.5}Cu_{32.5}P_{20}$	0.067	[19]
$Pd_{82}Si_{18}$	1.8×10^3	[40]
$Pd_{82}Si_{18}$	800	[41]
$Pd_{81}Si_{19}$ (with flux treatment)	6	[42]
$Zr_{65}Al_{7.5}Ni_{10}Cu_{17.5}$	1.5	[43]
$Zr_{41.2}Ti_{13.8}Cu_{12.5}Ni_{10.0}Be_{22.5}$	1.4	[44]
$Zr_{46.25}Ti_{8.25}Cu_{7.5}Ni_{10.0}Be_{27.5}$	28	[44]
$Zr_{57}Cu_{15.4}Ni_{12.6}Al_{10}Nb_5$	10	[45]

Glass formation

Retention of liquid phase

Formation of crystalline phases

Thermodynamical point

Small change in free E. (liq. → cryst.)

Kinetic point

Low nucleation and growth rates

Structural point

Highly packed random structure

Empirical rules

- (1) multi-component alloy system
- (2) significant difference in atomic size ratios
- (3) negative heats of mixing
- (4) close to a eutectic composition
- (5) compositions far from a Laves phase region

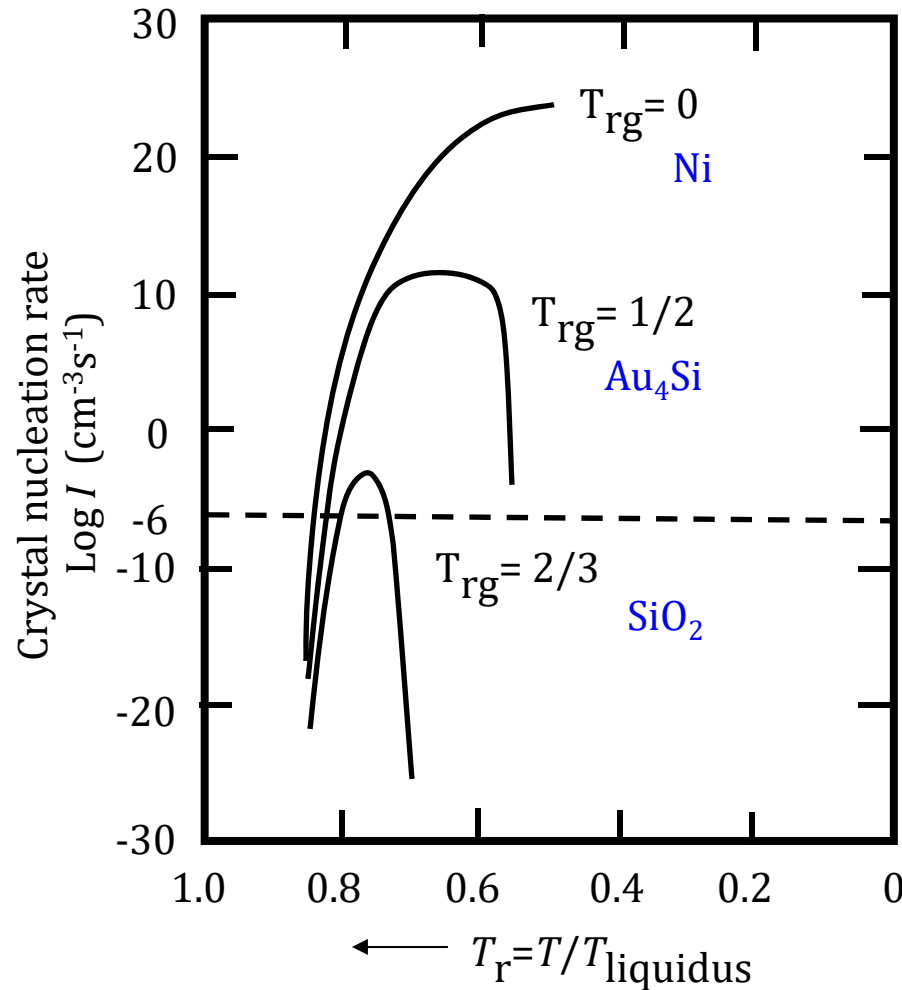
- **Higher degree of dense random packed structure**
- *Suppression* of nucleation and growth of crystalline phase



High glass-forming ability (GFA)

3.3 Reduced Class Transition Temperature (Kinetic aspect for glass formation)

T_{rg} parameter = $T_g/T_l \sim \eta$: the higher T_{rg} , the higher η , the lower R_c
 : ability to avoid crystallization during cooling



$$T_{rgNi} < T_{rgAu4Si} < T_{rgSiO2}$$

$$R_{Ni} > R_{Au4Si} > R_{SiO2}$$

Turnbull, 1959 ff.

- Based on the nucleation theory, Turnbull suggested that at $T_{rg} \geq 2/3$, homogeneous nucleation of the crystalline phase is completely suppressed. Most typically, a minimum value of $T_{rg} \sim 0.4$ has been found to be necessary for the glass to form.
- One should note the T_l , liquidus temperature as the point at the end of the liquid formation, and not at the beginning of melting.

TABLE 3.2

Reduced Glass Transition Temperatures (T_{rg}) for Different Glass-Forming Alloys

Alloy Composition	T_{rg}	References
$Ca_{65}Al_{35}$	0.69	[47]
$Ca_{67}Mg_{19}Cu_{14}$	0.60	[48]
$Ca_{57}Mg_{19}Cu_{24}$	0.64	[48]
$Cu_{65}Hf_{35}$	0.62	[49]
$Cu_{49}Hf_{42}Al_9$	0.62	[50]
$Cu_{64}Zr_{36}$	0.64	[51]
$La_{55}Al_{25}Ni_{20}$	0.71	[32]
$La_{62}Al_{15.5}(Cu,Ni)_{22.3}$	0.58	[52]
$La_{50.2}Al_{20.5}(Cu,Ni)_{29.3}$	0.47	[52]
$Ni_{62}Nb_{38}$	0.60	[37]
$Ni_{61}Nb_{33}Zr_6$	0.49	[53]
$Pd_{40}Ni_{40}P_{20}$	0.67	[54]
$Pd_{40}Cu_{30}Ni_{10}P_{20}$	0.67	[18,55]
$Zr_{41.2}Ti_{13.8}Cu_{12.5}Ni_{10}Be_{22.5}$	0.624	[45]
$Zr_{45.38}Ti_{9.62}Cu_{8.75}Ni_{10}Be_{26.25}$	0.50	[44]

- The concept of T_{rg}^* was introduced for kinetic reasons with the need to avoid crystallization [46]. It is known (and we will discuss this in some detail in Section 3.4) that T_g is a very weak function of the solute content, i.e., T_g varies much more slowly with solute concentration than the liquidus temperature, T_l . Consequently, the value of T_{rg} increases with increasing solute content, up to the eutectic composition, and therefore it becomes easier to avoid crystallization of the melt at the eutectic composition [13]. This reasoning seems to work well in simple binary alloy systems. But, in the case of multicomponent alloy systems such as the BMG compositions, the values of T_g and T_l vary significantly. Since the variation of viscosity with temperature is different for different alloy systems (and depends on whether a glass is strong or fragile), T_g alone may not provide information about the variation of viscosity with temperature and therefore, the T_{rg} criterion may not be valid in some systems.

Easy glass formation at compositions corresponding to high T_{rg} can be easily realized in alloy systems that feature deep eutectic reactions in their phase diagrams, and this is further explained in Section 3.4.

3.4 Deep Eutectics (Thermodynamic aspect for glass formation)

- High GFA : low free energy $\Delta G(T)$

for transformation of liquid to crystalline phase

$$\Delta G(T) = \Delta H_f - T\Delta S_f$$

$\Delta G \downarrow \rightarrow \Delta H_f \downarrow$ & $\Delta S_f \uparrow$
Enthalpy of fusion Entropy of fusion

$\Delta S_f \uparrow$: proportional to the number of microscopic states
Entropy of fusion

Multi-component alloy systems containing more than 3 elements
causes an increase in the degree of dense random packing

$\Delta H_f \downarrow$ **Large negative enthalpy of mixing** among constituent elements
Enthalpy of fusion

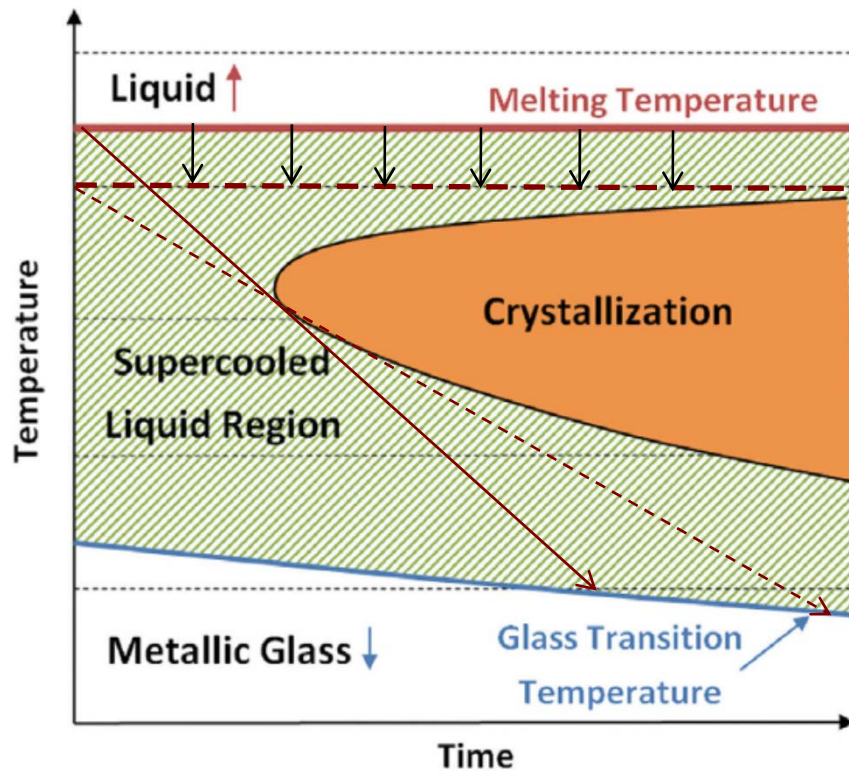
- * The free energy at a constant temperature also decreases in the cases of low chemical potential caused by **low enthalpy** and **high reduced glass transition temperature** ($=T_l/T_g$) and **high interface energy** between liquid and solid phase.

3.4 Deep Eutectics (Thermodynamic aspect for glass formation)

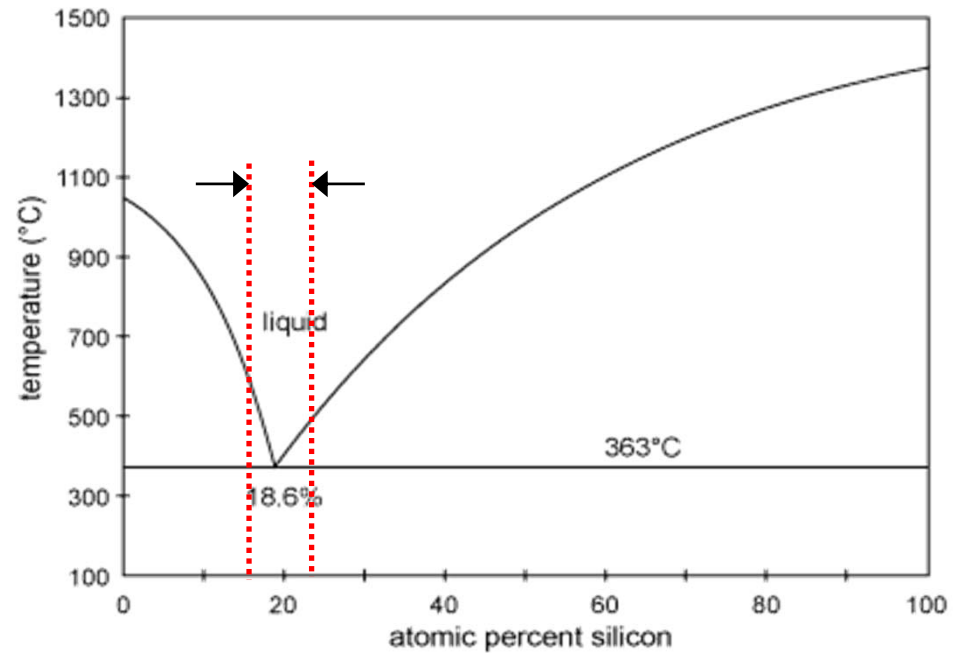
$\Delta H_f \downarrow \rightarrow$ deep eutectic condition: increase stability of stable liquid ($= T_g/T_l \uparrow$)

- decreasing melting point \rightarrow less supercooled at $T_g \rightarrow \Delta G = G^{liq} - G^{cryst} \downarrow$

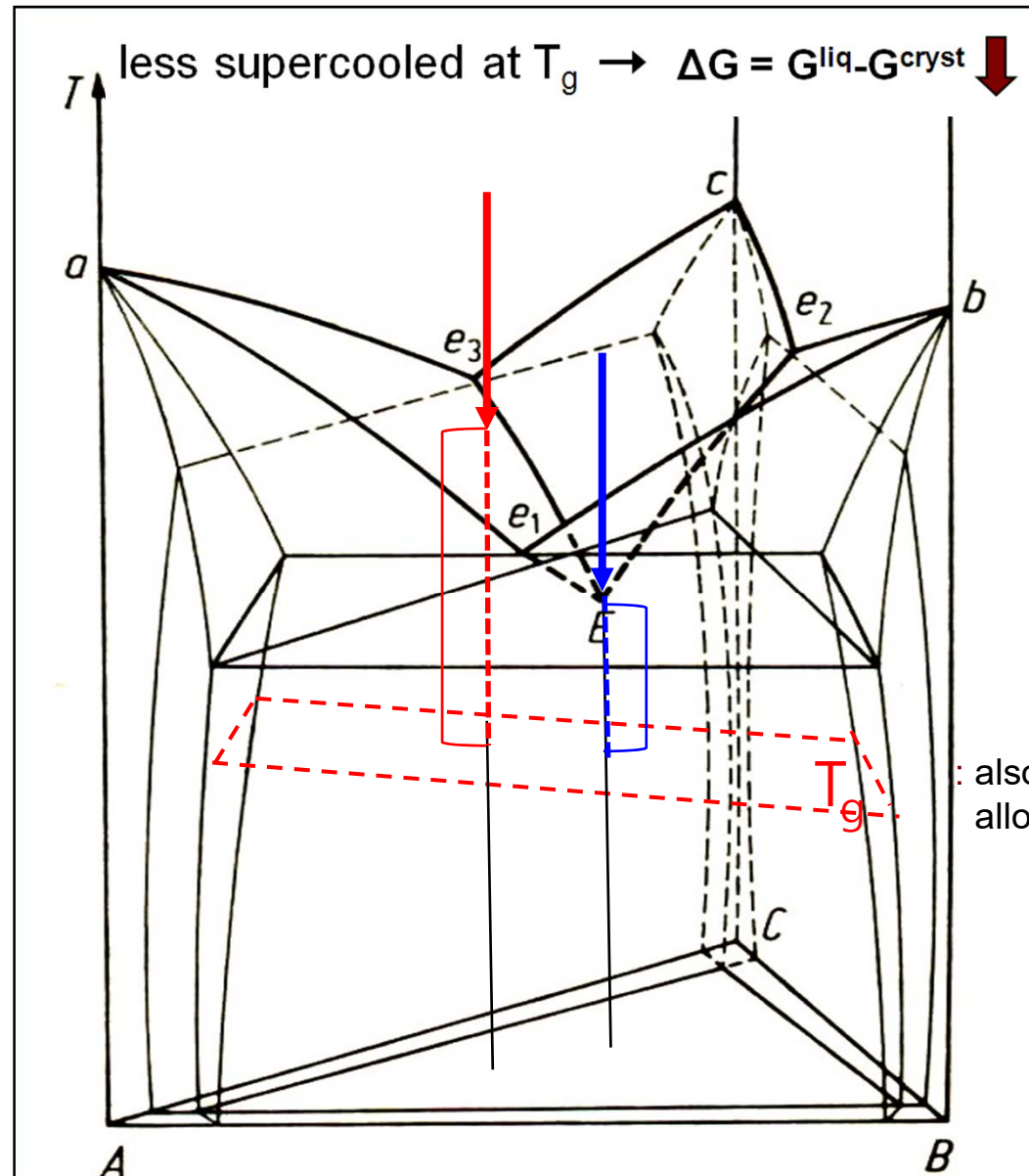
ex) metallic / inorganic system



Glass forming region:
Compositions near the eutectic



Multi-component eutectic alloys with strong negative heat of mixing



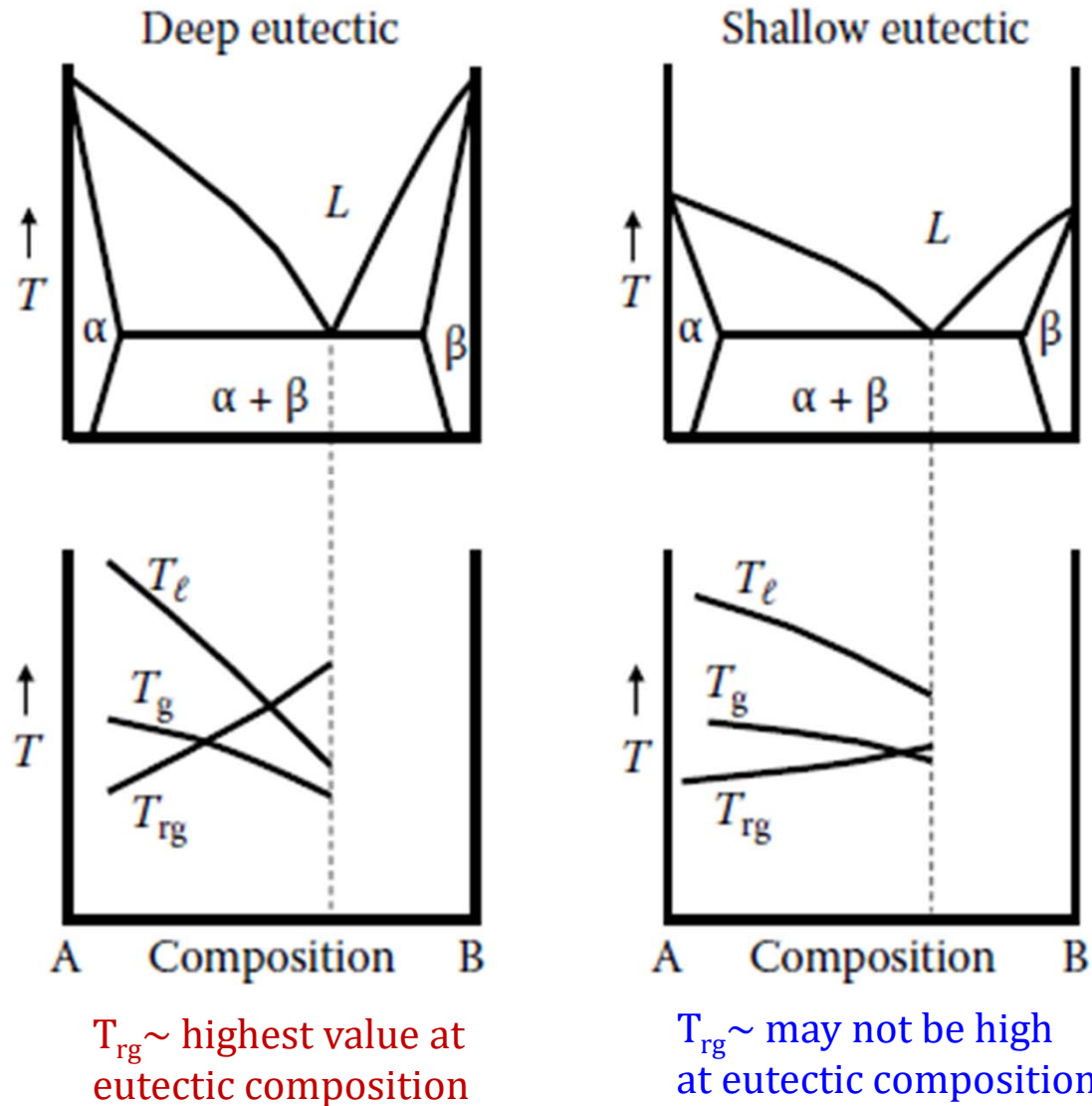


FIGURE 3.3

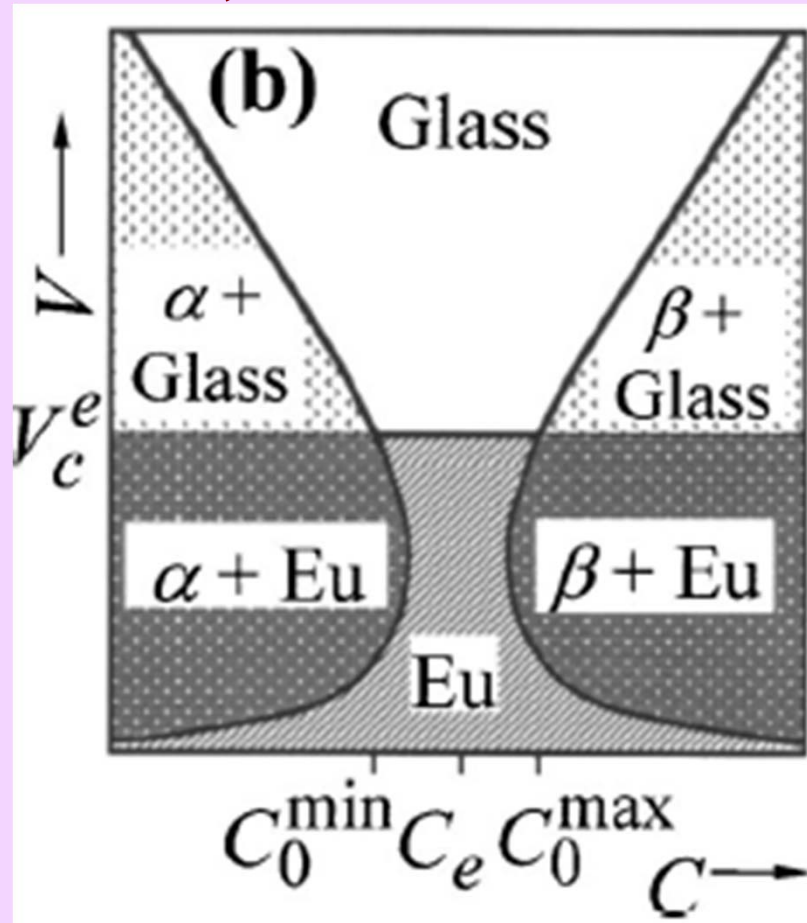
Schematic variation of the glass transition temperature, T_g , liquidus temperature, T_l , the reduced glass transition temperature, T_{rg} , in two different types of eutectic systems—deep eutectic and shallow eutectic.

Ribbons of about 20–50 μm in thickness were produced by melt-spinning techniques in a number of binary alloy systems near eutectic compositions and they were confirmed to be glassy. Some of the most investigated eutectic compositions are found in Fe–B, Pd–Si, Cu–Zr, Ni–Nb, Ni–Ta, etc., alloy systems [1,2]. There have been some reports in recent years of “bulk” (?) metallic glass synthesis in binary alloy systems such as Ca–Al [59], Cu–Hf [49], Cu–Zr [51], Ni–Nb [37], and Pd–Si [42]. But, the maximum diameters of these binary alloy glassy rods were only 1 or 2 mm, and even then, some of these alloy glasses contained nanocrystalline particles embedded in the glassy matrix [60]. This point will be further discussed in detail in later chapters. But, the

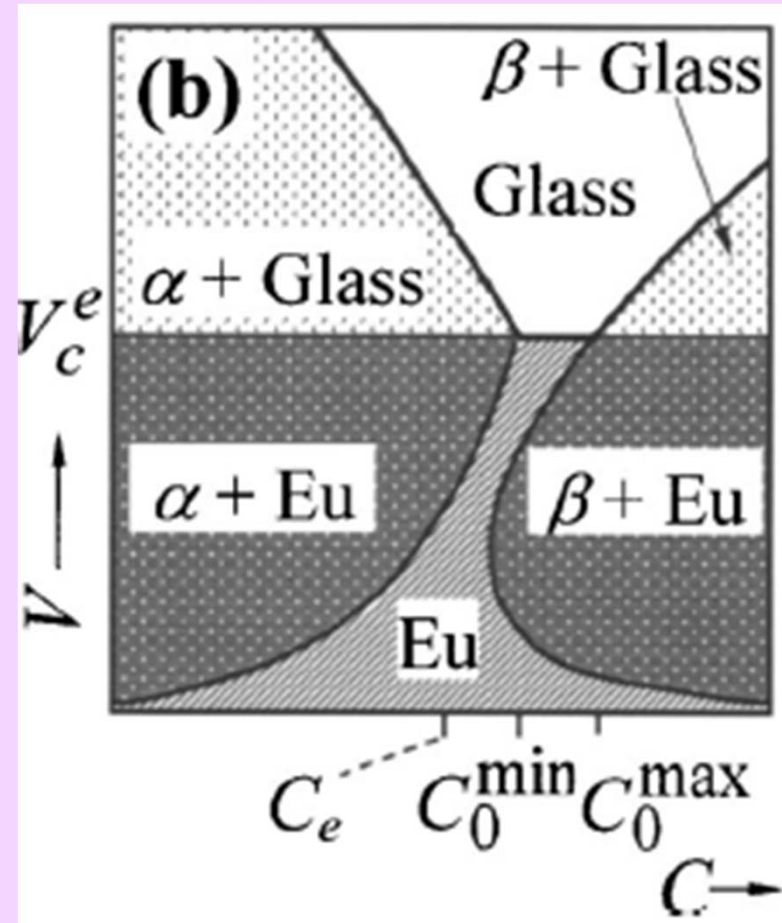
- important point here is that the “bulk” glassy phase is produced not at the eutectic composition, but, at off-eutectic compositions. Further, the highest GFA, i.e., the composition at which glass formation was the easiest or the maximum diameter of the BMG rod could be obtained, was located away from the eutectic composition. The best glass-forming compositions have been reported to be at 35 at.% Hf in Cu–Hf, 36 at.% Zr in Cu–Zr, 38 at.% Nb in Ni–Nb, and 19 at.% Si in Pd–Si alloy systems. But, the eutectic compositions in these alloy systems are at 33.0 and 38.6 at.% Hf in Cu–Hf, 38.2 at.% Zr in Cu–Zr, 40.5 at.% Nb in Ni–Nb, and 17.2 at.% Si in Pd–Si systems [61]. Similarly, it was reported that while a nearly fully glassy rod with 12 mm diameter could be obtained at an off-eutectic composition near $\text{La}_{62}\text{Al}_{15.7}(\text{Cu,Ni})_{22.3}$, only a 1.5 mm diameter rod could be obtained in a fully glassy condition for the eutectic alloy of $\text{La}_{66}\text{Al}_{14}(\text{Cu,Ni})_{20}$ [52].

Strategy for pinpointing the best glass-forming alloys

< Symmetric Eutectic >



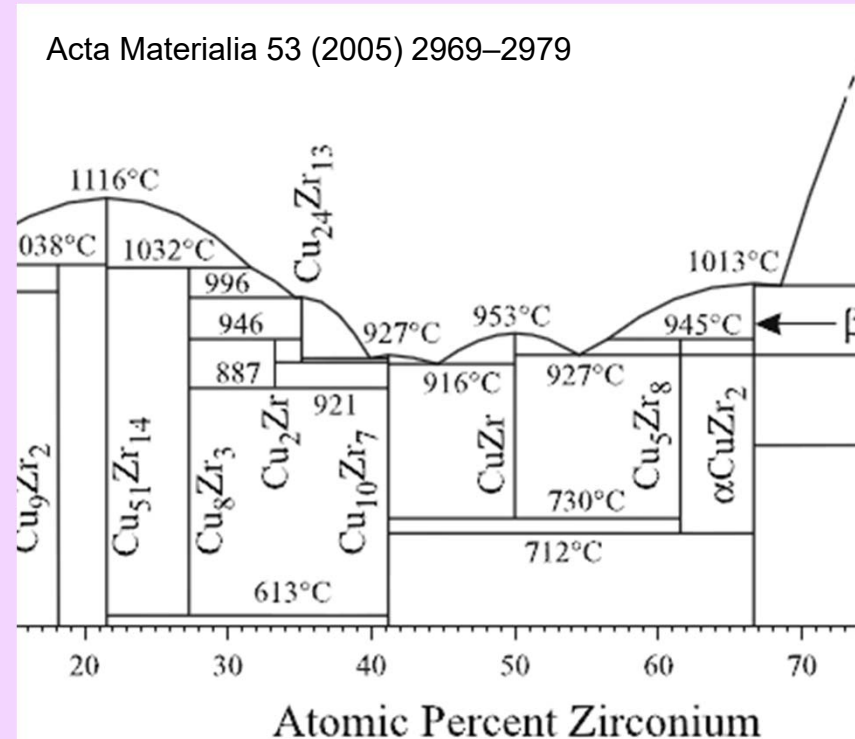
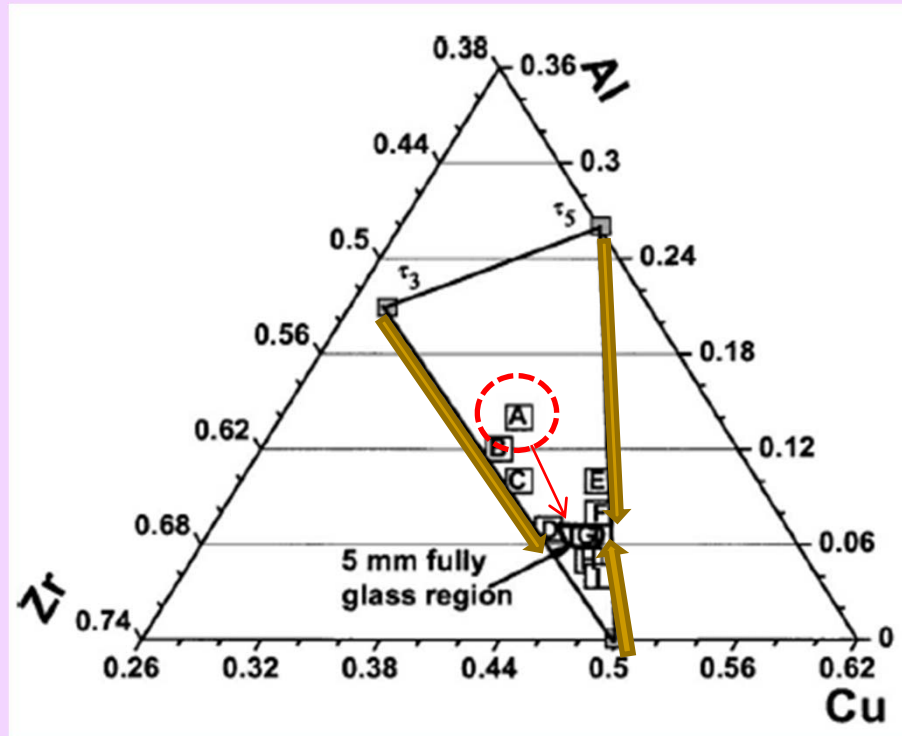
< Non-symmetric Eutectic >



► Glass region is located between composites with different 2nd phases.

➔ Useful to find the composition with maximum GFA

Composites & Glass forming composition

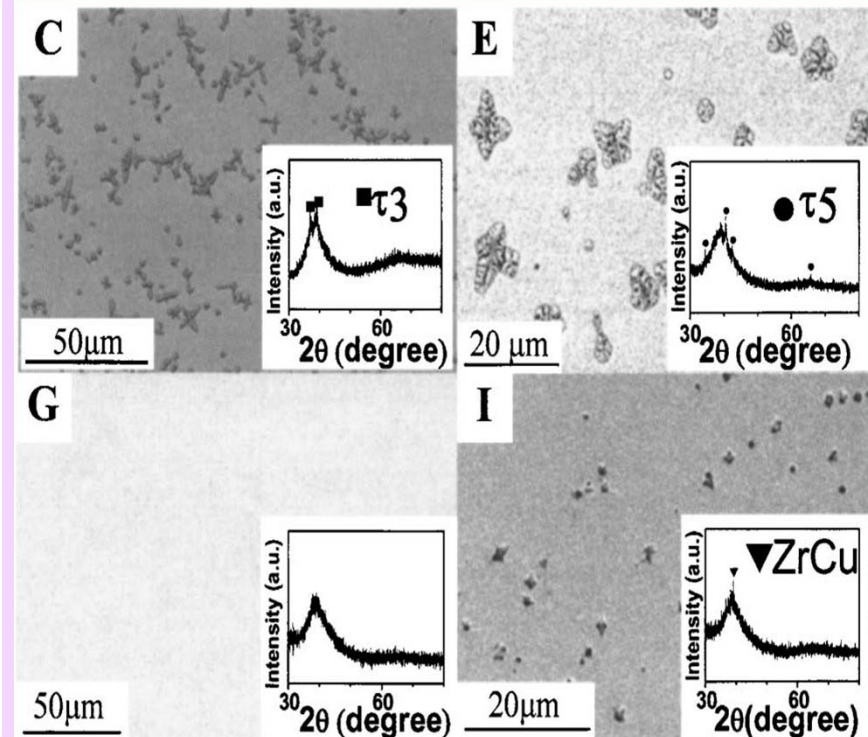
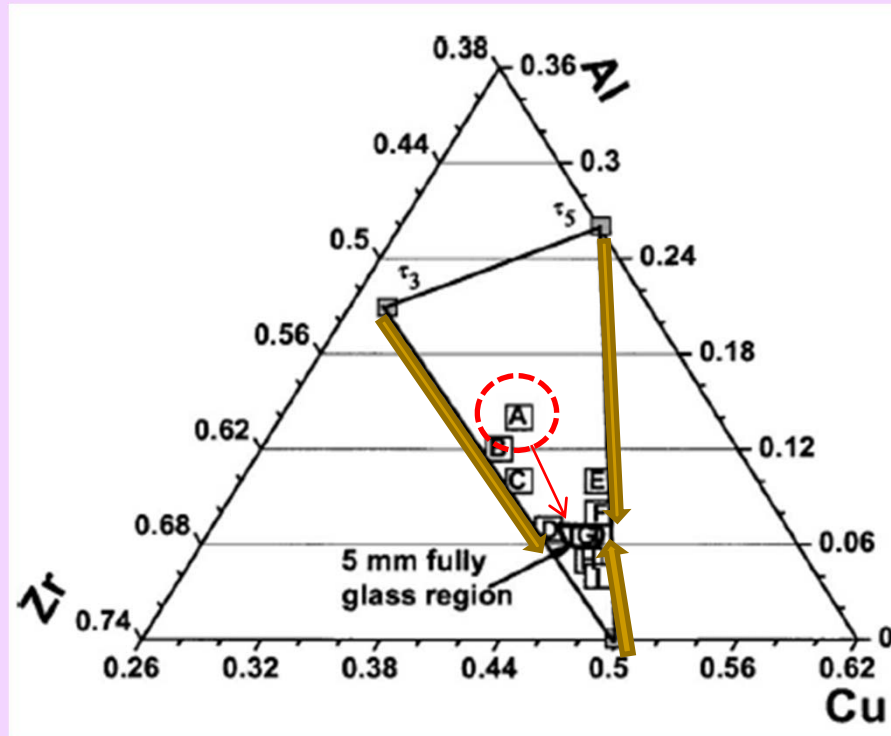


► Tie triangle among ZrCu , τ_3 , $\tau_5 \rightarrow A = \text{“ternary eutectic composition”}$

1. $A(\text{Zr}_{48}\text{Cu}_{38}\text{Al}_{14})$: eutectic composition but glass and composite X

➔ In Cu-Zr alloy, the composition with high GFA is moved to near liquidus line with higher slope of Zr-rich composition.

Composites & Glass forming composition



2. Three composition forming region (casted into 5 mm-diam copper mold)

Following arrows, τ_3 +glass (B,C,D), τ_5 glass (E,F), ZrCu + glass (I,H) ~

➔ At point G, competing crystalline phase changes

➔ G = Formation of fully glass

3.5 Topological Model (Structural aspect for glass formation)

Metallic glasses produced by RSP methods in the form of thin ribbons have been traditionally classified into two groups, viz., metal-metalloid and metal-metal types. Structural models of the metal-metalloid-type metallic glasses have identified that the best composition to form a glass is one that contains about 80 at.% of the metal component and 20 at.% of the metalloid component. The actual glass composition ranges observed are 75–85 at.% of the metal and 15–25 at.% of the metalloid. As stated in Chapter 2, the 80 at.% of the metal can be either a single transition metal or a combination of transition metals or one or a combination of noble metals. Similarly, the 20 at.% of the metalloid content could be made up of just one component or a mixture of a number of components. In the case of metal-metal types, however, there is no such restriction on compositions. Metal-metal-type metallic glasses have been observed to form over a wide range of compositions, starting from as low as 9 at.% of solute. Some typical compositions in which metal-metal type glasses have been obtained are $\text{Cu}_{25-72.5}\text{Zr}_{27.5-75}$, $\text{Fe}_{89-91}\text{Zr}_{9-11}$, $\text{Mg}_{68-75}\text{Zn}_{25-32}$, $\text{Nb}_{55}\text{Ir}_{45}$, and $\text{Ni}_{58-67}\text{Zr}_{33-42}$ [65].

* Metallic glass : Randomly dense packed structure

1) Atomic size difference: TM – metalloid (M, ex) Boron)

→ M is located at interior of the tetrahedron of four metal atoms (TM_4M)

→ denser  by increasing resistivity of crystallization, GFA 

→ Ex) Fe-B: tetrahedron with B on the center position

1) interstitial site, B= simple atomic topology

2) skeleton structure

3) bonding nature: close to covalent bonding

Irrespective of the actual size of the voids and whether the above model is valid or not, it is of interest to note that the metal-metalloid-type binary phase diagrams exhibit deep eutectics at around a composition of 15–25 at.% metalloid. Some typical examples are Fe–B (17 at.% B), Au–Si (18.6 at.% Si), and Pd–Si (17.2 at.% Si). Therefore, the concepts of deep eutectics and structural models also seem to converge in obtaining glasses in the (transition or noble) metal-metalloid types.

3.5.2. Egami and Waseda Criterion

One of the possible ways by which a crystalline metallic material can become glassy is by the introduction of lattice strain. The lattice strain introduced disturbs the crystal lattice and once a critical strain is exceeded, the crystal becomes destabilized and becomes glassy. In fact, Egami takes pains to state that “In general, alloying makes glass formation easier, not because alloying stabilizes a glass, but because it destabilizes a crystal” [72, p. 576]. Using the atomic scale elasticity theory, Egami and Waseda [73] calculated the atomic level stresses in the solid solution (the solute atoms are assumed to occupy the substitutional lattice sites in the solid solution) and the glassy phase. They observed that in a glass, neither the local stress fluctuations nor the total strain energy vary much with solute concentration, when normalized with respect to the elastic moduli. But, in a solid solution, the strain energy was observed to increase continuously and linearly with solute content. Thus, beyond a critical solute concentration, the glassy alloy becomes energetically more favorable than the corresponding crystalline lattice. From the vast literature available on the formation of binary metallic glasses obtained by RSP methods, the authors noted that a minimum solute concentration was necessary in a binary alloy system to obtain the stable glassy phase by RSP methods.

2) min. solute content, C_B^* : empirical rule

By Egami & Waseda: in A-B binary system

$$C_B^{\min} \left| \frac{(v_B - v_A)}{v_A} \right| = C_B^{\min} \left| \left(\frac{r_B}{r_A} \right)^3 - 1 \right| \approx 0.1$$

v : atomic volume
 A : matrix, B : solute

minimum concentration of B for glass formation

→ Inversely proportional to atomic volume mismatch

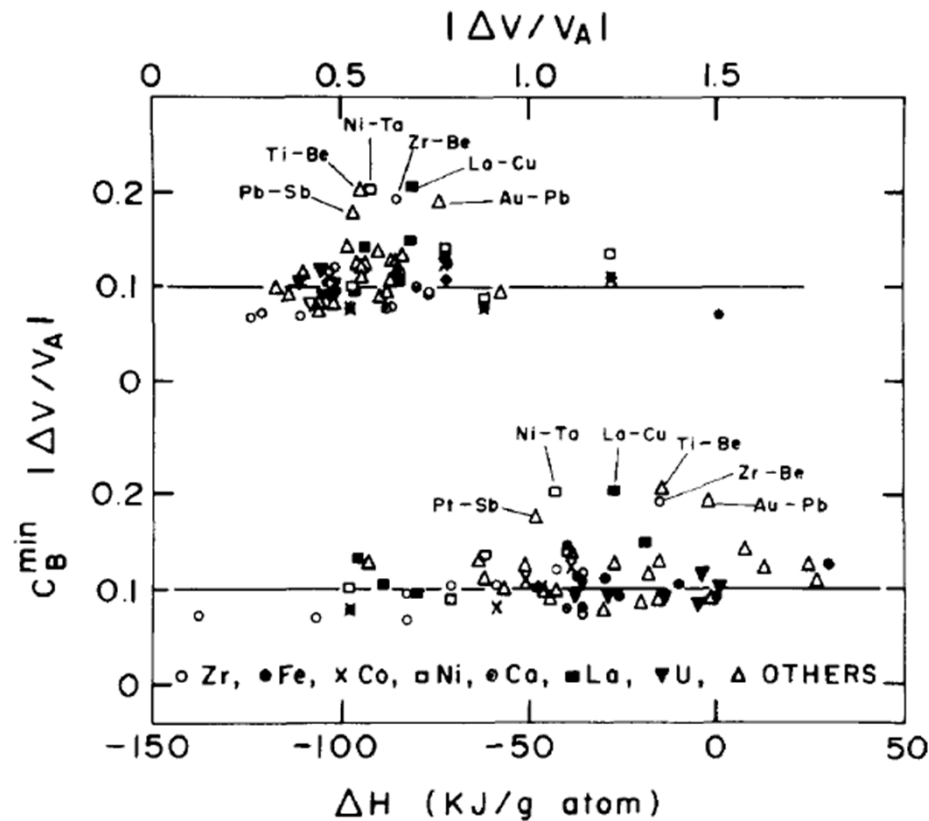


Fig. 1. Relation between $|\lambda_0| = C_B^{\min} |\Delta v/v_A|$, and $|\Delta v/v_A|$ and ΔH , for 66 binary systems which can be vitrified by liquid quenching.

3.5.3. Nagel and Tauc Criterion

Nagel and Tauc [74,75] proposed that a glass is most likely to form if its electronic energy lies in a local metastable minimum with respect to composition change. They showed that if the structure factor corresponding to the first strong peak of the diffuse scattering curve, K_p , satisfies the relationship $K_p = 2 k_F$, where k_F is the wave vector at the Fermi energy, then the electronic energy does indeed occupy a local minimum.

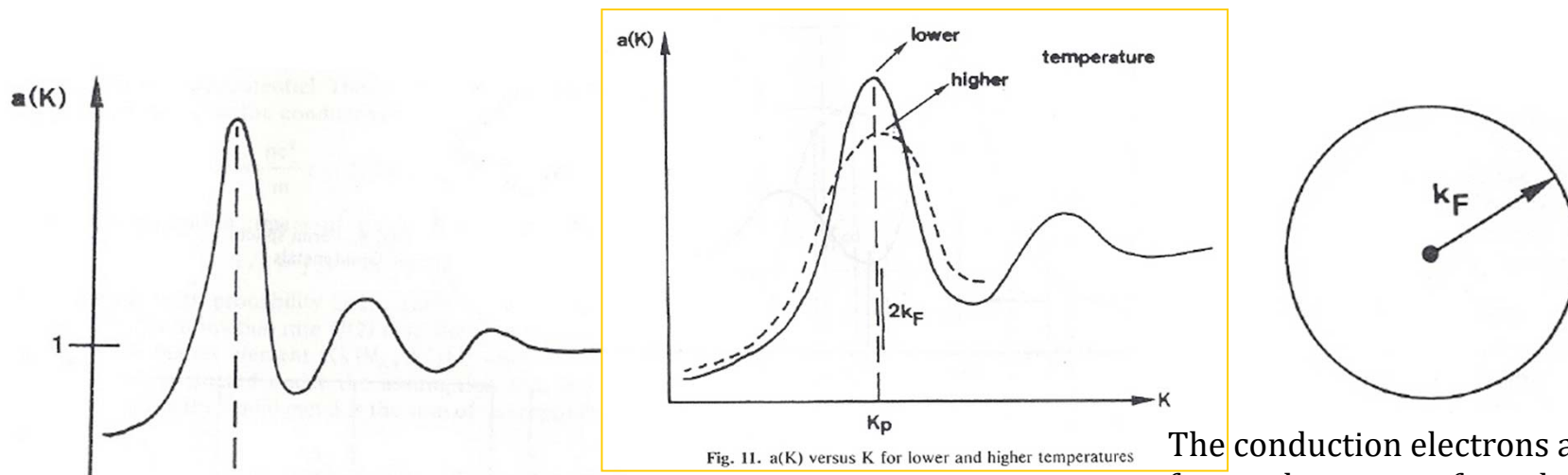


Fig. 7. Schematic structure factor $a(K)$

Fig. 11. $a(K)$ versus K for lower and higher temperatures

$$K_p = 2 k_F$$

The conduction electrons are supposed to form a degenerate free-electron gas with a spherical Fermi surface.

$$2K_F = 2(3\pi^2 n)^{1/3} = 2 \left(\frac{3\pi^2}{eR_H} \right)^{1/3}$$

$a(K)$ Fourier transform of the pair correlation function $g(r)$

K_p Nearest neighbor distance of the liquid metal in K -space

: Diameter of Fermi surface

3.6 Bulk Metallic Glasses

Since 1989, intense research has been carried out in synthesizing and characterizing BMGs with a section thickness or diameter of a few millimeters to a few centimeters.

First, phase diagrams are not available for the multicomponent alloy systems. Therefore, we do not know where the eutectic compositions lie, and much less about deep eutectics.

Additionally, because the number of components is really large, determining the minimum solute content will be a formidable problem since the contribution of each component to the volumetric strain is going to be different depending on their atomic sizes.

Therefore, newer criteria have been proposed to explain glass formation in BMGs in view of the large number of components present.

3.7 Inoue Criteria – Empirical Rules

1. The alloy must contain at least three components. The formation of glass becomes easier with increasing number of components in the alloy system.

a) Thermodynamic point of view

Since the value of ΔS_f can be significantly increased by increasing the number of components in the alloy, it has been relatively easy to produce BMGs in multicomponent alloys. Since an increase in ΔS_f also leads to an increase in the degree of the dense random packing of atoms, this results in a decrease in ΔH_f and also an increase in the solid–liquid interfacial energy, σ . Both these factors contribute to a decrease in the free energy of the system.

b) Kinetic point of view

Since the equation for homogeneous nucleation rate for the formation of crystalline nuclei from a supercooled melt (Equation 2.4) contains η , α , and β , control of these parameters can lead to a reduction in the nucleation rate. For example, a reduction in ΔH_f , and an increase in σ and/or ΔS_f can be achieved by an increase in α and β values. This, in turn, will decrease the nucleation rate and consequently promote glass formation. An increase in the viscosity of the melt will also lead to a reduction in both nucleation and growth rates.

3.7 Inoue Criteria – Empirical Rules

2. A significant atomic size difference should exist among the constituent elements in the alloy. It is suggested that the atomic size differences should be above about 12% among the main constituent elements.

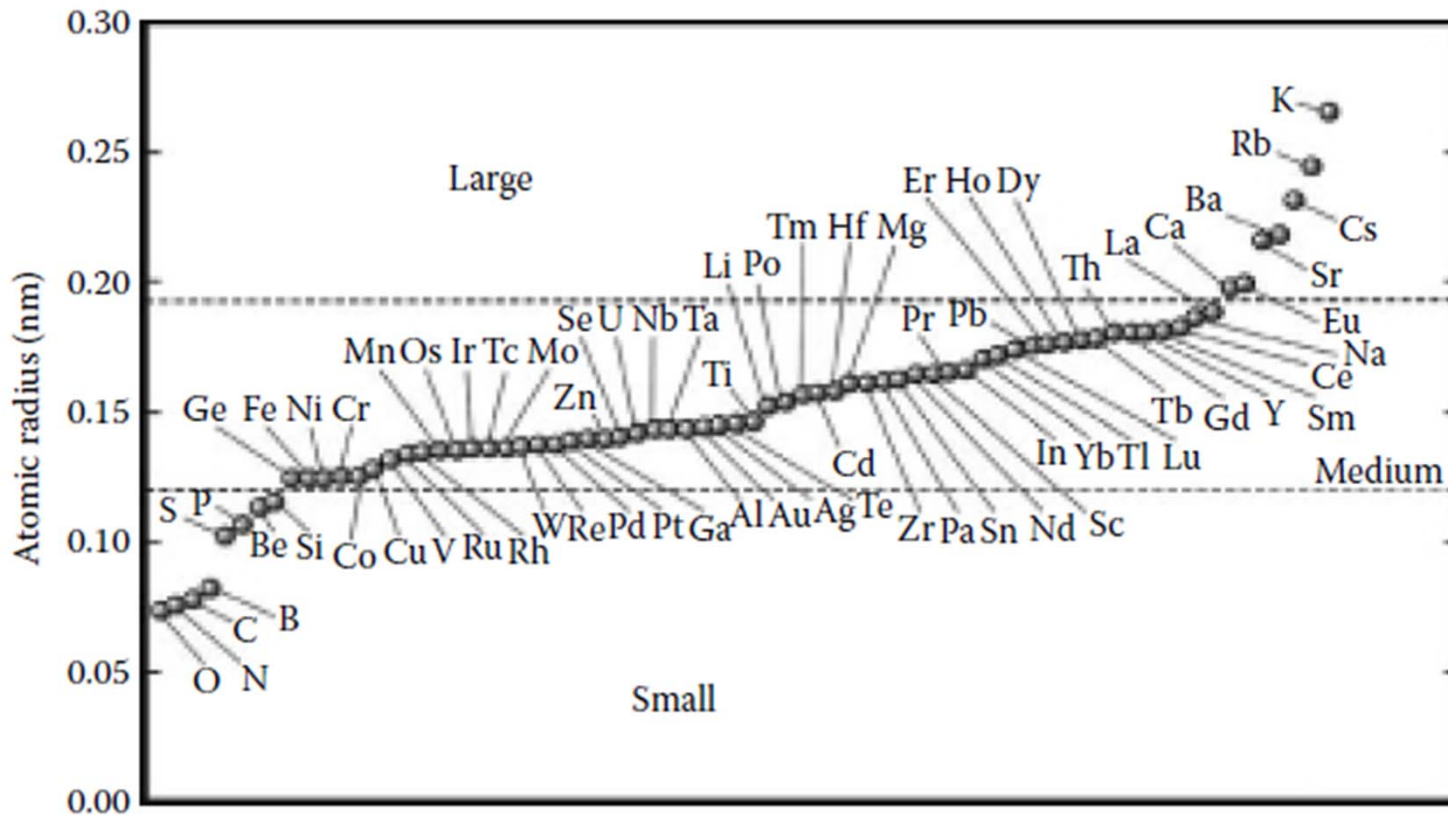
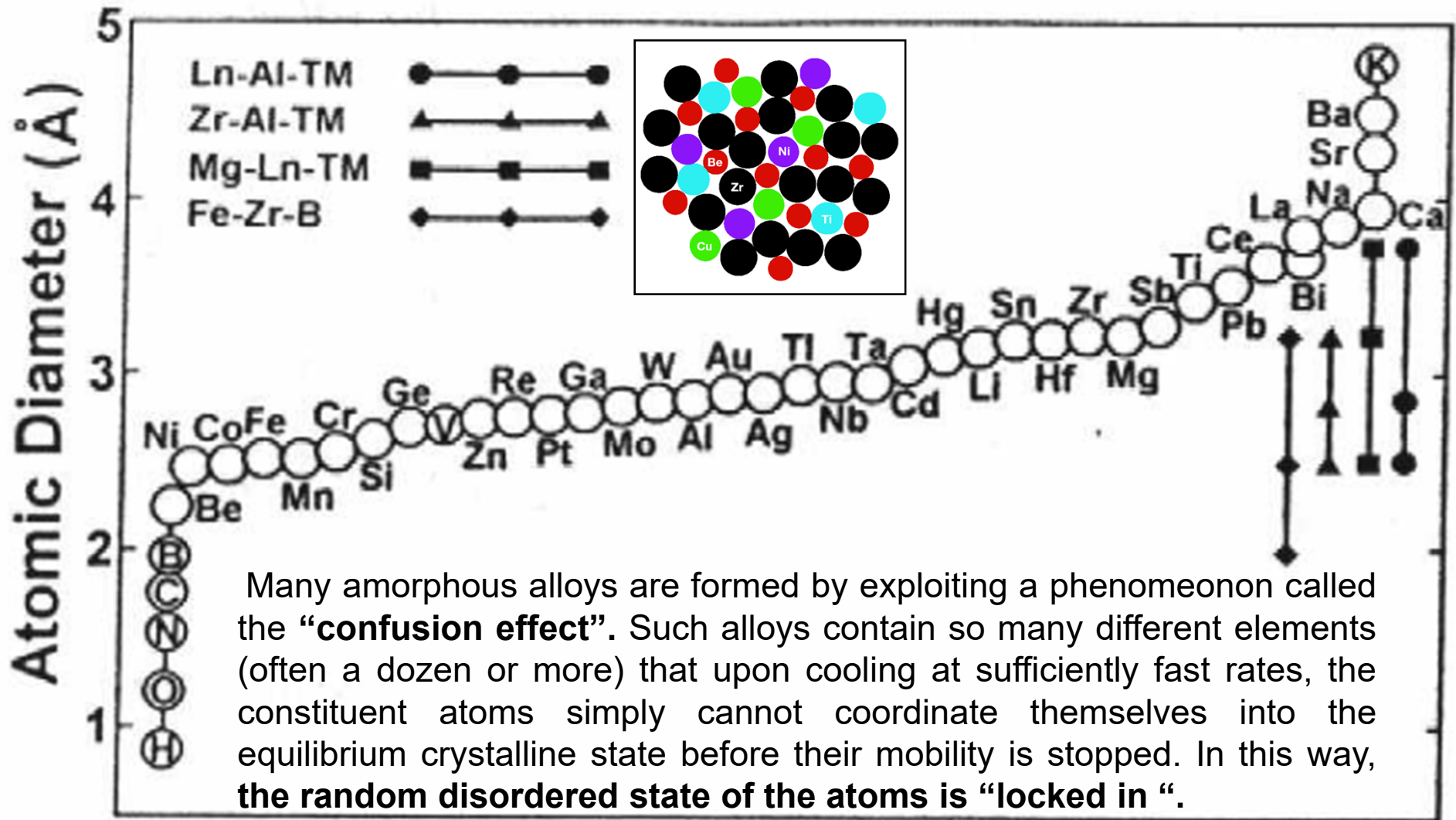


FIGURE 3.4

Atomic diameters of the elements that constitute bulk metallic glasses. These can be classified into three major groups of large, medium, and small sizes.

< significant difference in atomic size ratios >



3.7 Inoue Criteria – Empirical Rules

- There should be negative heat of mixing among the (major) constituent elements in the alloy system.

The combination of the significant differences in atomic sizes between the constituent elements and the negative heat of mixing is expected to result in efficient packing of clusters (see Section 3.12.2) and consequently increase the density of random packing of atoms in the supercooled liquid state. This, in turn, leads to increased liquid–solid interfacial energy, σ and decreased atomic diffusivity, both contributing to enhanced glass formation.

Table 3.3

Nearest Neighbor Distances (r) and Coordination Numbers (N) of the Different Atomic Pairs in a Glassy $Zr_{60}Al_{15}Ni_{25}$ Alloy Both in the As-Quenched and Crystallized States

Condition		r_1 (nm)	N_{Zr-Ni}	r_2 (nm)	N_{Zr-Zr}	N_{Zr-Al}
As-quenched	(a)	0.267 ± 0.002	2.3 ± 0.2	0.317 ± 0.002	10.3 ± 0.7	-0.1 ± 0.9
	(b)	0.267 ± 0.002	2.1 ± 0.2	—	—	—
	(c)	0.269 ± 0.002	2.3 ± 0.2	—	—	—
Crystallized	(a)	0.268 ± 0.002	3.0 ± 0.2	0.322 ± 0.002	8.2 ± 0.7	0.8 ± 0.9
	(b)	0.267 ± 0.002	3.0 ± 0.2	—	—	—
	(c)	0.273 ± 0.002	2.3 ± 0.2	—	—	—

Significant change in the coordination # of Zr-Al atomic pairs on crystallization
 → This suggests that there is necessity for long-range diffusion of Al atoms around Zr atoms during crystallization, which is difficult to achieve due to the presence of dense randomly packed clusters.

Source: Matsubara, E. et al., *Mater. Trans. JIM*, 33, 873, 1992. With permission.

Notes: Data from (a) ordinary radial distribution function (RDF), (b) conventional RDFs for Zr, and (c) conventional RDFs for Ni. “—” means that no values were given in the original publication.

The presence of dense randomly packed atomic configurations in the glassy state of BMGs can also be inferred from the small changes in the relative densities of the fully glassy and the corresponding fully crystalline alloys (see Table 6.1). It is noted that the densities of the glassy alloys are lower than those in the crystallized state. The difference between the fully glassy and fully crystalline alloys is typically about 0.5%, but is occasionally as high as 1% (see, for example, Ref. [81]). Further, the density difference between the structurally relaxed and fully glassy states is about 0.11%–0.15%. Thus, the small density differences between the glassy and crystallized conditions suggest that the glassy alloys contain dense randomly packed clusters in them.

Glass formation

Retention of liquid phase

Formation of crystalline phases

Thermodynamical point

Small change in free E. (liq. → cryst.)

Kinetic point

Low nucleation and growth rates

Structural point

Highly packed random structure

Empirical rules

- (1) multi-component alloy system
- (2) significant difference in atomic size ratios
- (3) negative heats of mixing
- (4) close to a eutectic composition
- (5) compositions far from a Laves phase region

- **Higher degree of dense random packed structure**
- *Suppression* of nucleation and growth of crystalline phase

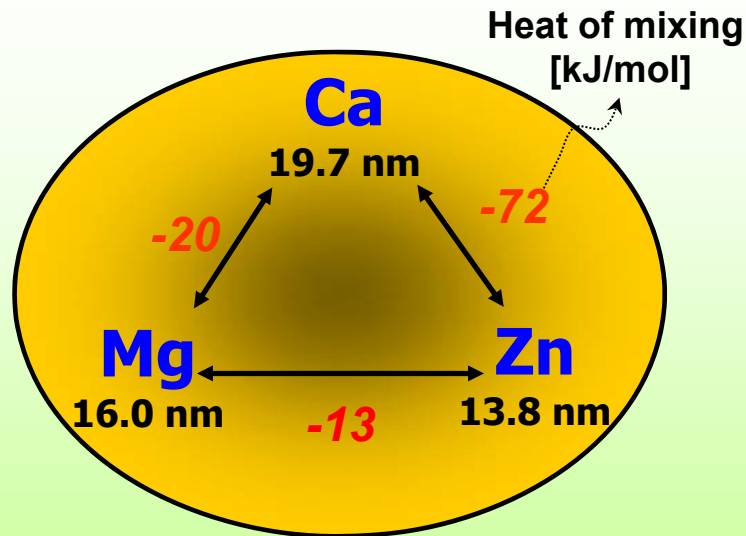


High glass-forming ability (GFA)

Alloy design and new BMG development

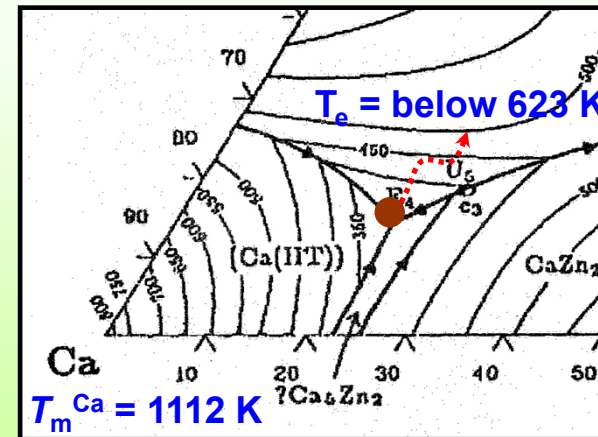
Ca-Mg-Zn alloy system

- Dense packed structure



- Large difference in atomic size
- Large negative heat of mixing

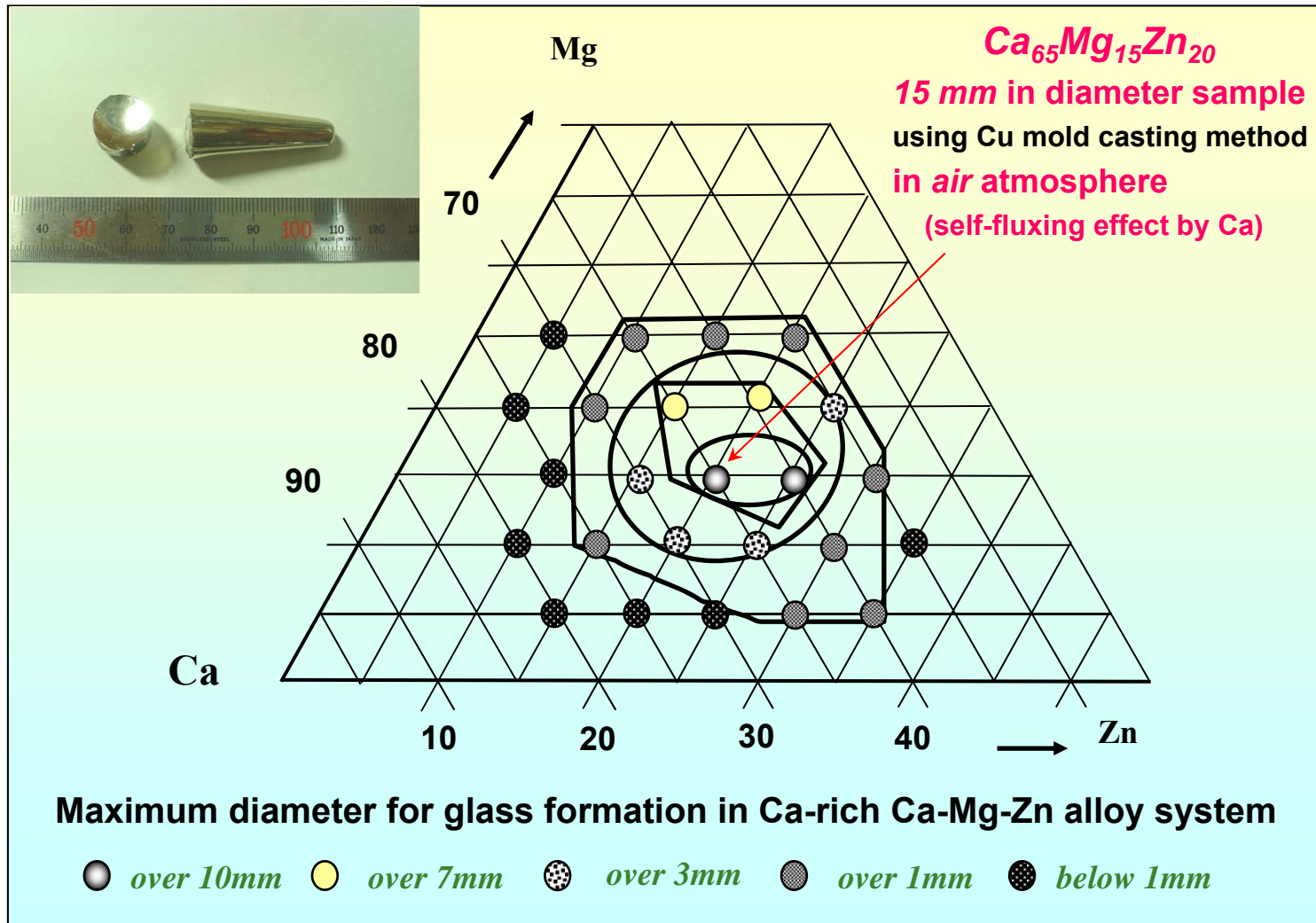
- Decrease of melting temp.



Deep eutectic condition

$$T_e / T_m^{\text{Ca}} = 0.560$$

Ca-Mg-Zn alloy system



* J. Mater. Res. 19, 685 (2004)

* Mater. Sci. Forum 475-479, 3415 (2005)

3.8 Exceptions to the Above Criteria

3.8.1 Less Than Three Components in an Alloy System – Binary BMGs

One of the apparent exceptions to this empirical rule appears to be that BMGs have been produced in binary alloy systems such as Ca–Al [59], Cu–Hf [49], Cu–Zr [51], Ni–Nb [37], and Pd–Si [42].

Two important points:

- 1) The maximum diameter of the glassy rods obtained in these binary alloys is relatively small, i.e. a maximum of only about 2 mm.
- 2) The “glassy” rods of the binary BMG alloys often seem to contain some nanocrystalline phases. (?)

Even though glassy (BMG) alloys of 1 or 2 mm diameter are produced in binary alloy compositions., their GFA improves dramatically with the addition of a third component. This observation again proves that a minimum of three components is required to produce a BMG alloy with a reasonably large diameter.

Hattori et al. [90] had conducted very careful high-pressure experiments on elemental Zr and Ti using a newly developed in situ angle-dispersive XRD using a two-dimensional detector and x-ray transparent anvils. These authors noted that despite the disappearance of all the Bragg peaks in the one-dimensional energy-dispersive data, two-dimensional angle-dispersive data showed several intense Bragg spots even at the conditions where amorphization was reported in these two metals. This investigation clearly confirms that pure metals cannot be amorphized

3.8.2 Negative Heat of Mixing

Phase separation is generally expected to occur in alloy systems containing elements that exhibit a positive heat of mixing. This is indicated by the presence of a miscibility gap in the corresponding phase diagram. Therefore, if phase separation has occurred, one immediately concludes that the constituent elements have a positive heat of mixing

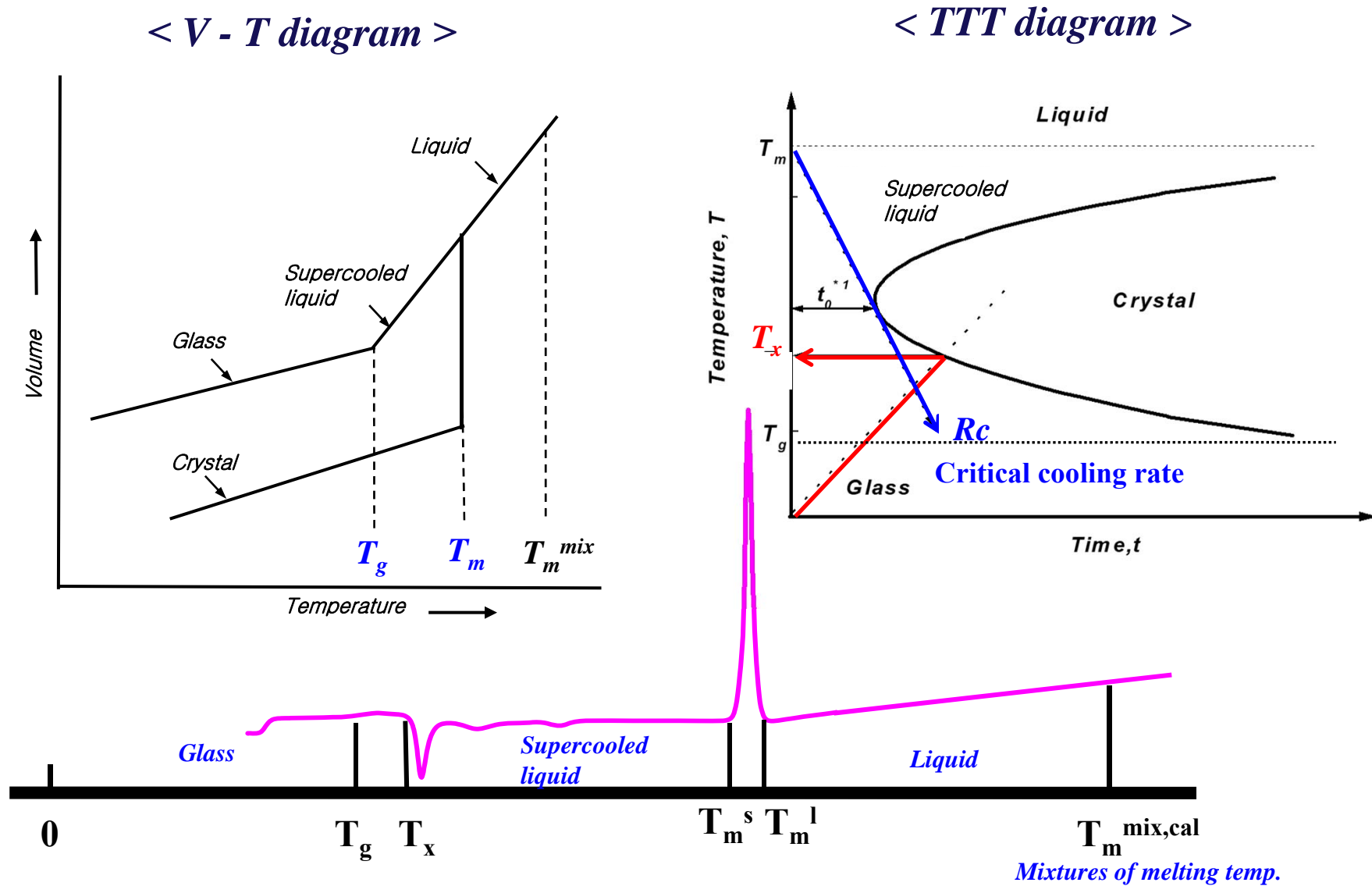
It has been suggested that it is theoretically possible to observe phase separation in alloy systems containing three or more elements, even though the heat of mixing is negative between any two elements in the alloy system. According to Meijering [94,95], a ternary alloy phase, consisting of components A, B, and C, can decompose into two phases with different compositions even when the enthalpy of mixing between any two components is negative. This is possible when the enthalpy of mixing, ΔH for one of the three possible binary alloy systems is significantly more negative than the others. For example, it is possible that in a ternary alloy system A–B–C, ΔH_{A-B} is much more negative than $\Delta H_{B-C} \approx \Delta H_{A-C}$. This argument suggests that a miscibility gap could be present in a ternary (or higher-order) BMG alloy system even when all the constituent elements have a negative enthalpy of mixing. In other words, phase separation is possible even in an alloy with a reasonably good GFA.

3.9 New Criteria: to develop better and more precise criteria to predict the GFA of alloy systems

All the new criteria that have been proposed in recent years to explain the high GFA of BMGs can be broadly grouped into the following categories:

1. *Transformation temperatures of glasses.* In this group, the GFA is explained on the basis of the characteristic transformation temperatures of the glasses such as T_g , T_x , and T_l , and the different combinations of these three parameters.
2. *Thermodynamic modeling.* Thermodynamic parameters such as heat of mixing are used in this group to predict the glass formation and evaluate GFA in a given alloy system.
3. *Structural and topological parameters.* In this group, consideration is given to the atomic sizes of the constituent elements, their electronegativity, electron-to-atom ratio, heat of mixing, etc. Majority of the work in this area has been due to Egami [107] and Miracle [108,109].
4. *Physical properties of alloys.* This group considers the physical properties of materials such as the viscosity of the melt, heat capacity, activation energies for glass formation and crystallization, bulk modulus, etc.
5. *Computational approaches.* These methods help in predicting the GFA of alloys from basic thermodynamic data [110,111], and without the necessity of actually conducting any experiments to synthesize the glass and determine the GFA.

3.10 Transformation Temperatures of Glasses



Representative GFA Parameters

Based on thermal analysis (T_g , T_x and T_l): thermodynamic and kinetic aspects

$$T_{rg} = T_g/T_l$$

D. Turnbull et al., *Contemp. Phys.*, 10, 473 (1969)

$$K = (T_x - T_g) / (T_l - T_x)$$

A. Hruby et al., *Czech.J.Phys.*, B22, 1187 (1972)

$$\Delta T^* = (T_m^{mix} - T_l) / T_m^{mix}$$

I. W. Donald et al., *J. Non-Cryst. Solids*, 30, 77 (1978)

$$\Delta T_x = T_x - T_g$$

A. Inoue et al., *J. Non-Cryst. Solids*, 156-158, 473 (1993)

$$\gamma = T_x / (T_l + T_g)$$

Z.P. Lu and C. T. Liu, *Acta Materialia*, 50, 3501 (2002)

Based on thermodynamic and atomic configuration aspects

$$\sigma = \Delta T^* \times P'$$

E. S. Park et al., *Appl. Phys. Lett.*, 86, 061907 (2005)

ΔT^* : Relative decrease of melting temperature + P' : atomic size mismatch

: can be calculated simply using data on melting temp. and atomic size

GFA Parameters on the basis of thermodynamic or kinetic aspects :

1) ΔT_x parameter = $T_x - T_g$

- quantitative measure of glass stability toward crystallization upon reheating the glass above T_g : stability of glass state
- cannot be considered as a direct measure for GFA

2) K parameter = $(T_x - T_g) / (T_l - T_x) = \Delta T_x / (T_l - T_x)$

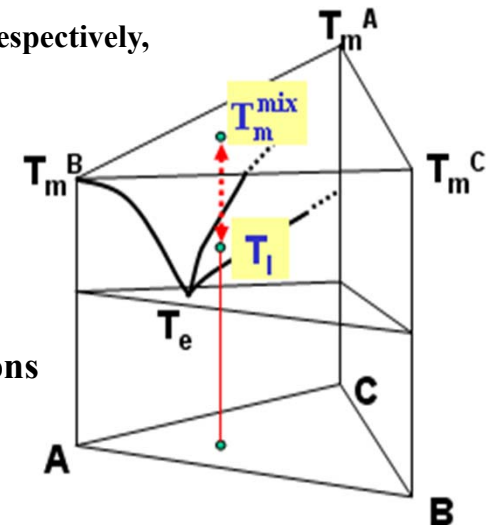
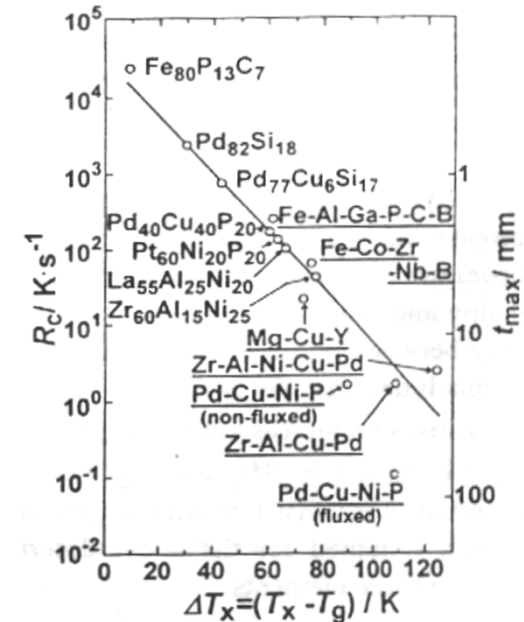
- based on thermal stability of glass on subsequent reheating
- includes the effect of T_l , but similar tendency to ΔT_x

3) ΔT^* parameter = $(T_m^{mix} - T_l) / T_m^{mix}$

$$- T_m^{mix} = \sum_i^n n_i \cdot T_m^i \quad (\text{where } n_i \text{ and } T_m^i \text{ are the mole fraction and melting point, respectively, of the } i \text{th component of an } n\text{-component alloy.})$$

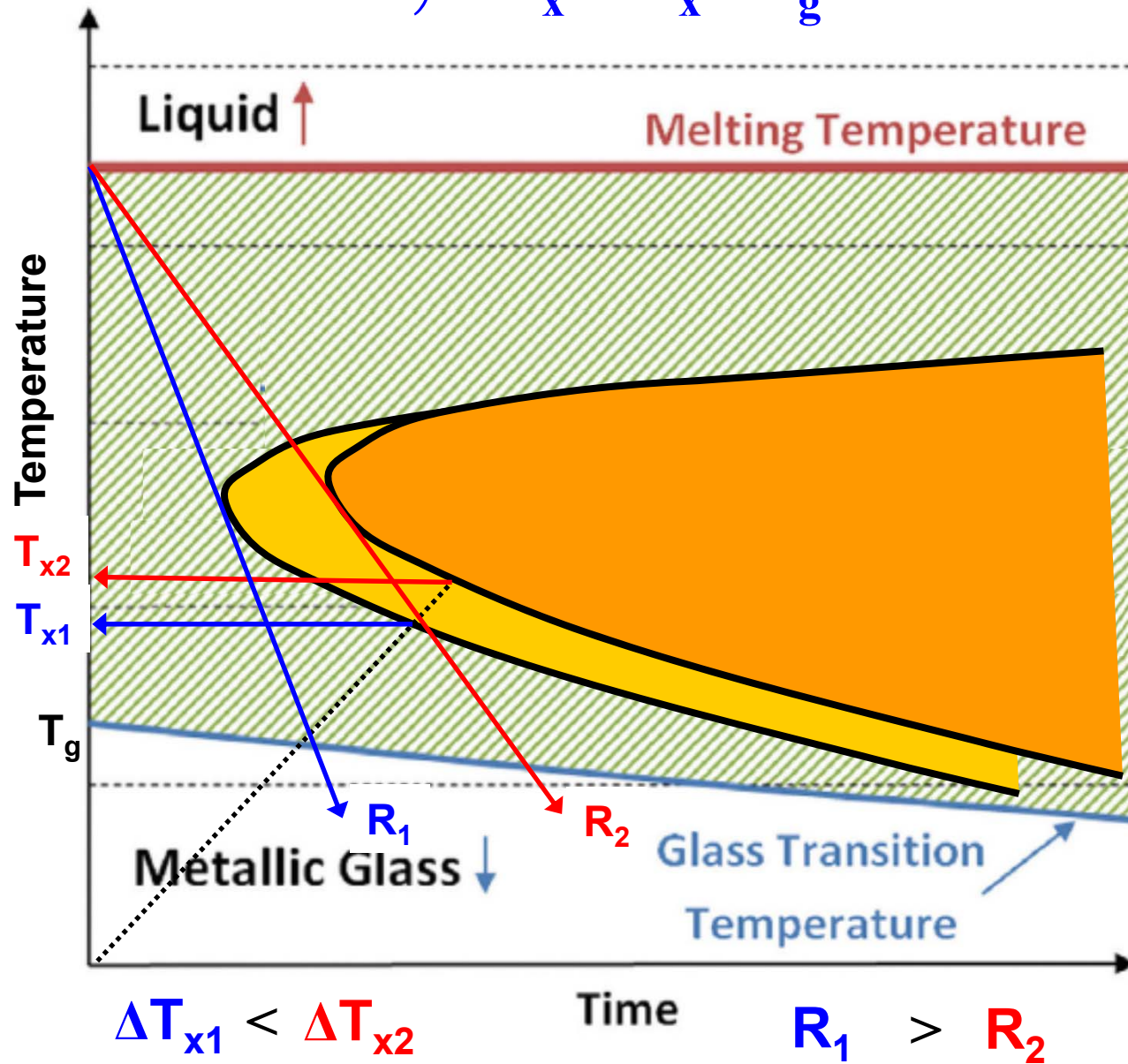
- evaluation of the stability of the liquid at equilibrium state
- alloy system with deep eutectic condition ~ good GFA
- for multi-component BMG systems: insufficient correlation with GFA

➔ T_m^{mix} represents the fractional departure of T_m with variation of compositions and systems from the simple rule of mixtures melting temperature



Time Temperature Transformation diagram:

$$1) \Delta T_x = T_x - T_g$$



From the above discussion, it is clear that the description of the GFA of alloys using the ΔT_x parameter as a criterion has not been found universally applicable in all situations and for all alloy systems. Some exceptions have been certainly noted. But, it should, however, be emphasized in this context that this was one of the most successful parameters in the early years of research on BMGs.

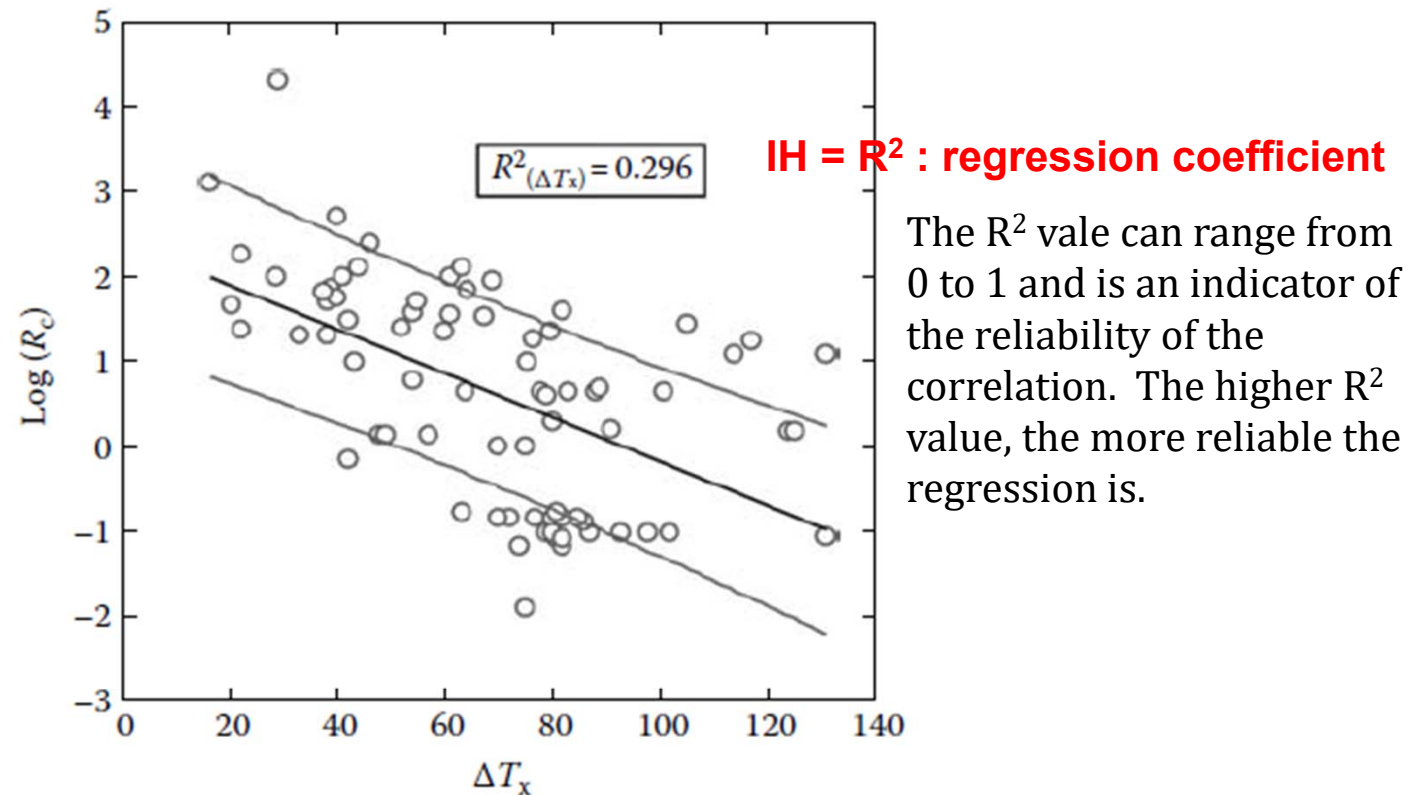


FIGURE 3.5

Variation of the critical cooling rate, R_c with the width of the supercooled liquid region, ΔT_x for a number of multicomponent bulk metallic glasses. Data for some of the binary and ternary metallic glasses reported earlier are also included for comparison.

GFA Parameters on the basis of thermodynamic or kinetic aspects :

1) ΔT_x parameter = $T_x - T_g$

- quantitative measure of glass stability toward crystallization upon reheating the glass above T_g : stability of glass state
- cannot be considered as a direct measure for GFA

2) K parameter = $(T_x - T_g)/(T_l - T_x) = \Delta T_x / (T_l - T_x)$

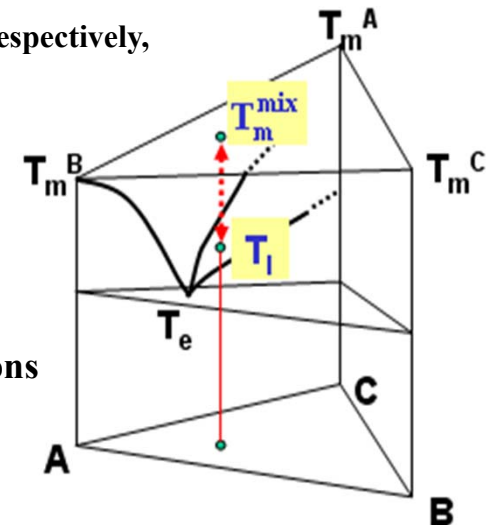
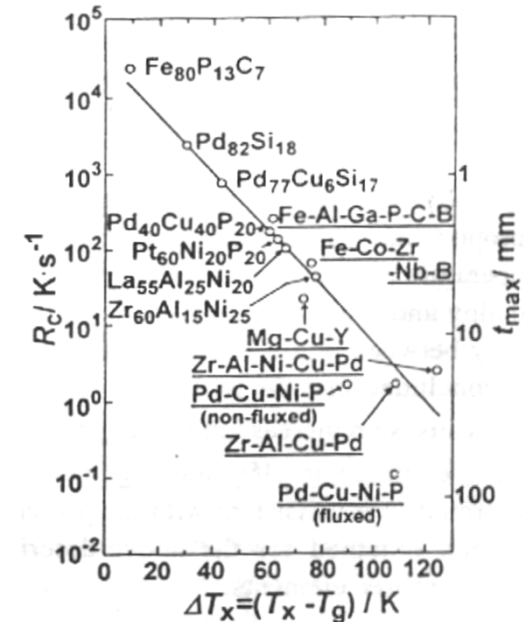
- based on thermal stability of glass on subsequent reheating
- includes the effect of T_l , but similar tendency to ΔT_x

3) ΔT^* parameter = $(T_m^{mix} - T_l) / T_m^{mix}$

- $T_m^{mix} = \sum_i^n n_i \cdot T_m^i$ (where n_i and T_m^i are the mole fraction and melting point, respectively, of the i th component of an n -component alloy.)

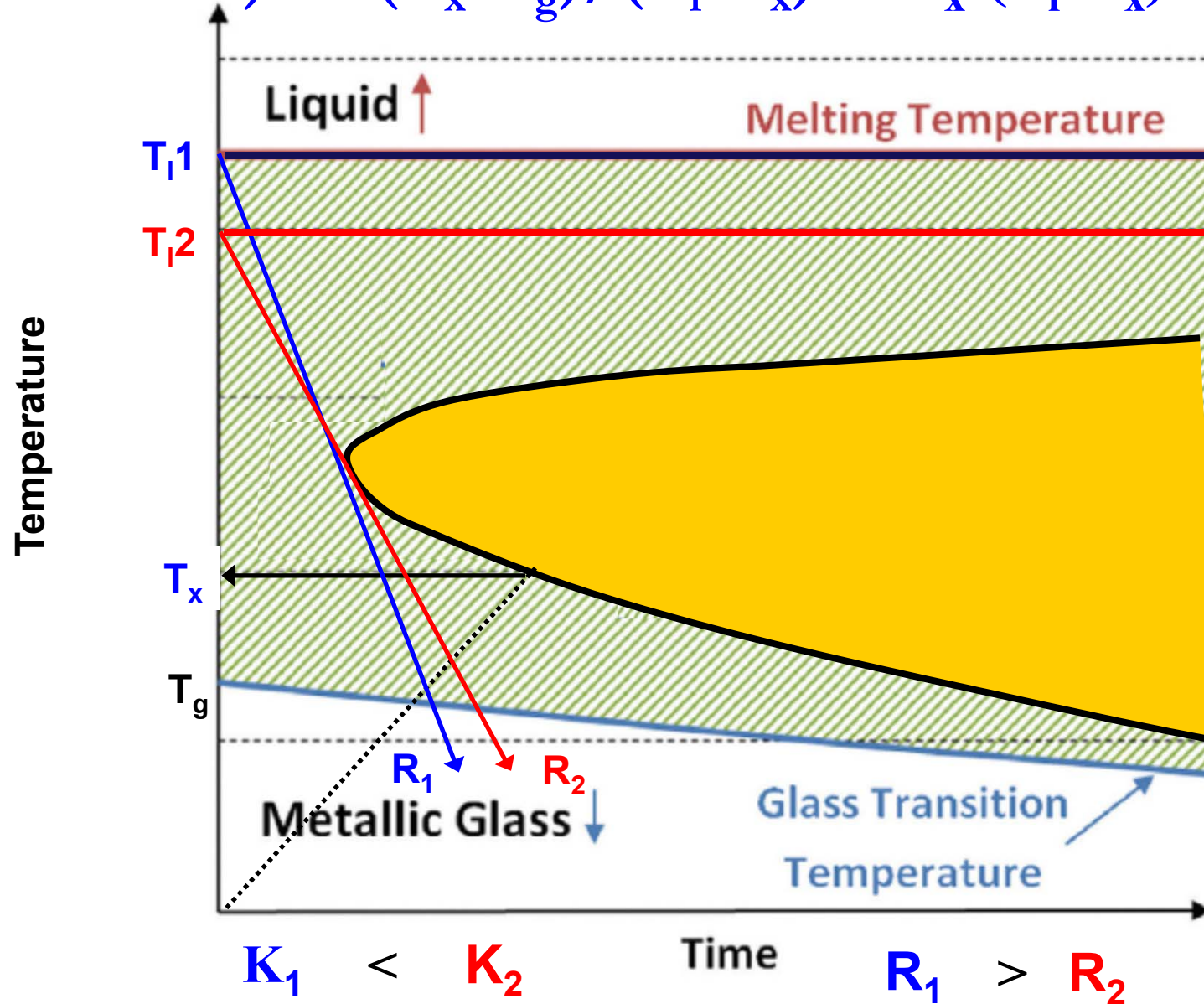
- evaluation of the stability of the liquid at equilibrium state
- alloy system with deep eutectic condition ~ good GFA
- for multi-component BMG systems: insufficient correlation with GFA

➔ T_m^{mix} represents the fractional departure of T_m with variation of compositions and systems from the simple rule of mixtures melting temperature



Time Temperature Transformation diagram:

$$2) K = (T_x - T_g) / (T_l - T_x) = \Delta T_x / (T_l - T_x)$$



GFA Parameters on the basis of thermodynamic or kinetic aspects :

1) ΔT_x parameter = $T_x - T_g$

- quantitative measure of glass stability toward crystallization upon reheating the glass above T_g : stability of glass state
- cannot be considered as a direct measure for GFA

2) K parameter = $(T_x - T_g) / (T_l - T_x) = \Delta T_x / (T_l - T_x)$

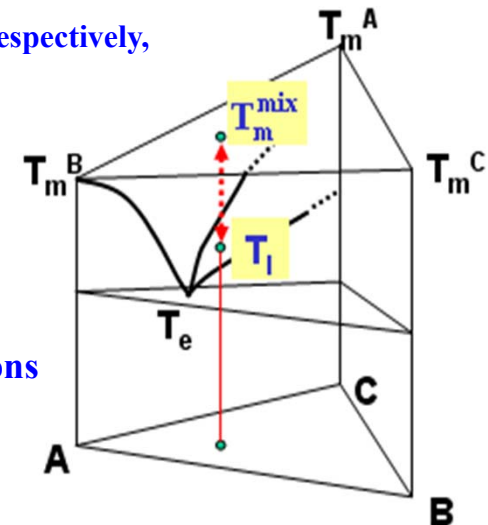
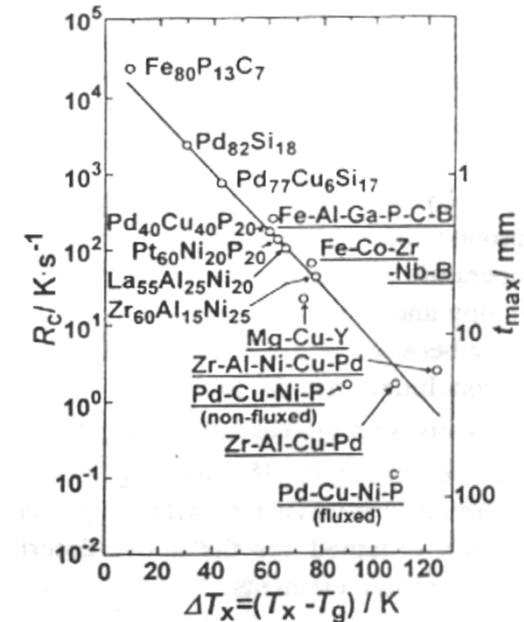
- based on thermal stability of glass on subsequent reheating
- includes the effect of T_l , but similar tendency to ΔT_x

3) ΔT^* parameter = $(T_m^{mix} - T_l) / T_m^{mix}$

$$T_m^{mix} = \sum_i^n n_i \cdot T_m^i \quad (\text{where } n_i \text{ and } T_m^i \text{ are the mole fraction and melting point, respectively, of the } i \text{ th component of an } n\text{-component alloy.})$$

- evaluation of the stability of the liquid at equilibrium state
- alloy system with deep eutectic condition ~ good GFA
- for multi-component BMG systems: insufficient correlation with GFA

➔ T_m^{mix} represents the fractional departure of T_m with variation of compositions and systems from the simple rule of mixtures melting temperature



☀ Relative decrease of melting temperature

: ratio of Temperature difference between liquidus temp. T_l and imaginary melting temp. T_m^{mix} to T_m^{mix}

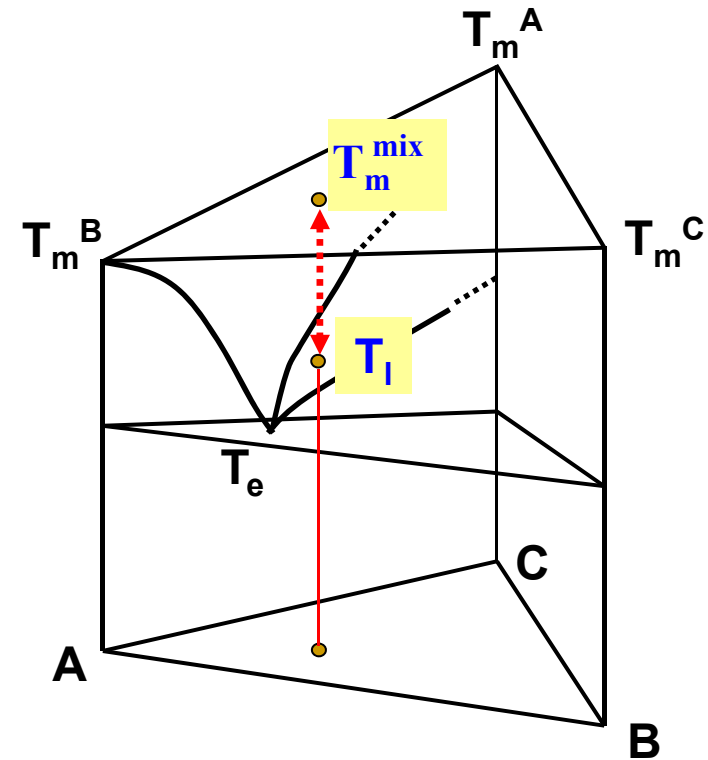
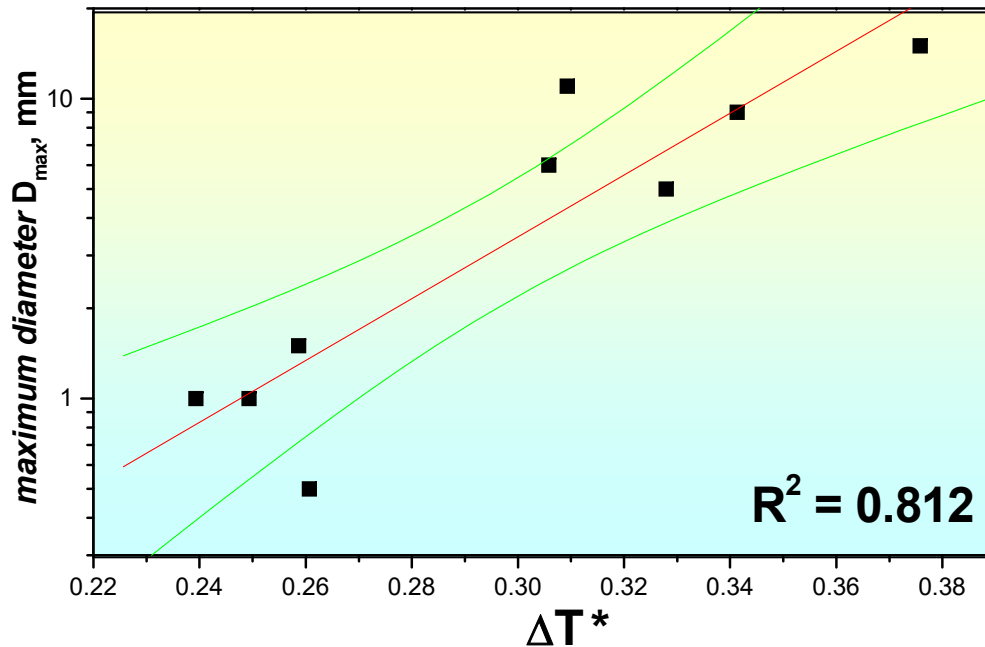
(where, $T_m^{mix} = \sum x_i T_m^i$, $x_i = \text{molefraction}$, $T_m^i = \text{melting point}$)

$$\Delta T^* = \frac{T_m^{mix} - T_l}{T_m^{mix}}$$

by I.W. Donald et al. (*J. Non-Cryst. Solids*, 30, 77 (1978))

➡ $\Delta T^* \geq 0.2$ in most of glass forming alloys

Ca-Mg-Zn alloy system



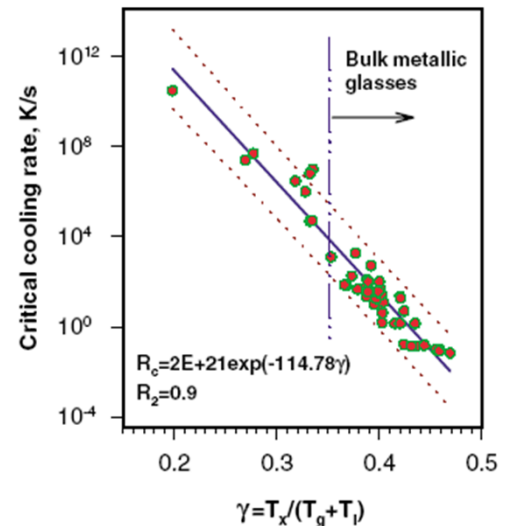
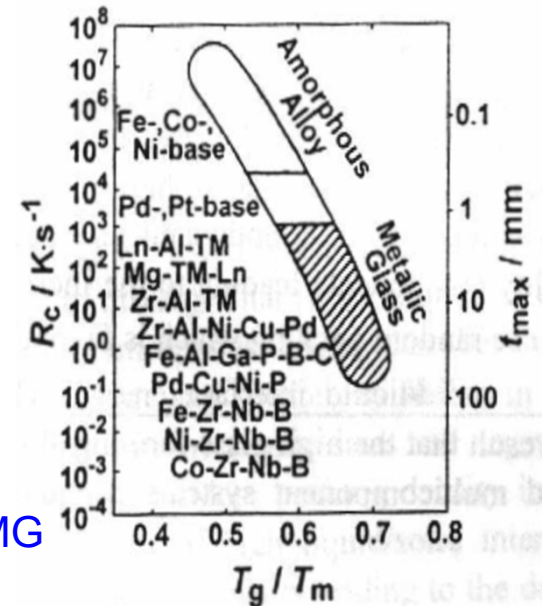
GFA Parameters on the basis of thermodynamic or kinetic aspects :

4) T_{rg} parameter = T_g/T_l

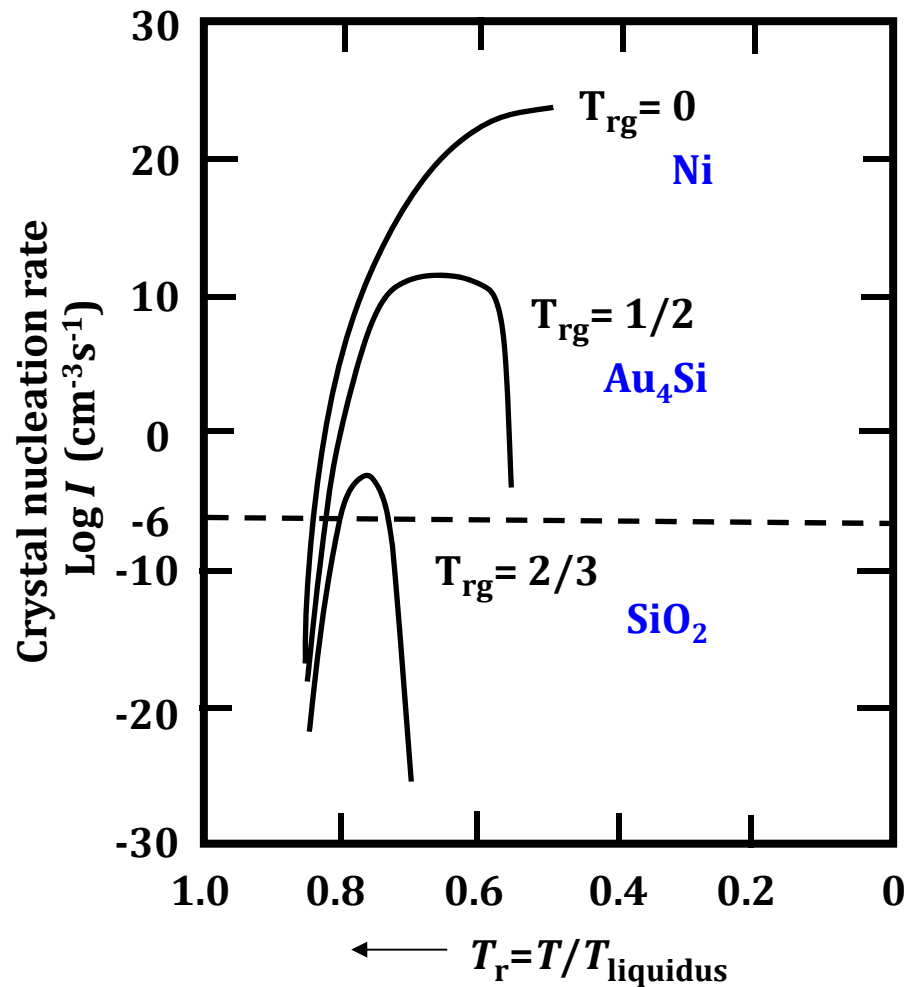
- kinetic approach to avoid crystallization before glass formation
- Viscosity at T_g being constant, the higher the ratio T_g/T_l , the higher will be the viscosity at the nose of the CCT curves, and hence the smaller R_c
- $T_l \downarrow$ and $T_g \uparrow$ \blacktriangleright lower nucleation and growth rate \blacktriangleright GFA \uparrow
 - significant difference between T_l and T_g in multi-component BMG
 - insufficient information on temperature-viscosity relationship
 - ▶ insufficient correlation with GFA

5) γ parameter = $T_x / (T_l + T_g)$

- thermodynamic and kinetic view points - relatively reliable parameter
- stability of equilibrium and metastable liquids: T_l and T_g
- resistance to crystallization: T_x



T_{rg} parameter = $T_g/T_l \sim \eta$: the higher T_{rg} , the higher η , the lower R_c
 : ability to avoid crystallization during cooling



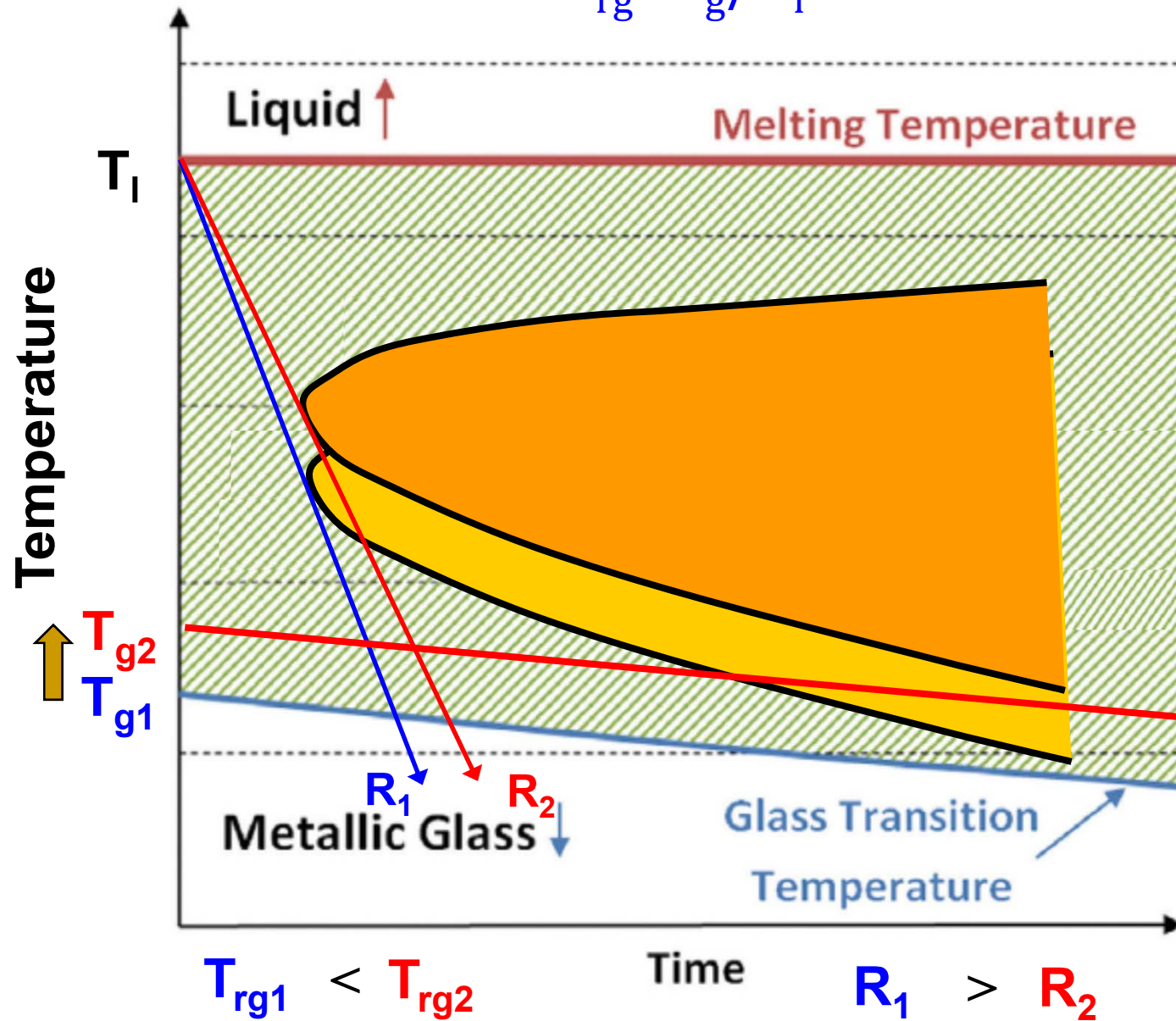
$$T_{rgNi} < T_{rgAu4Si} < T_{rgSiO2}$$

$$R_{Ni} > R_{Au4Si} > R_{SiO2}$$

Turnbull, 1959 ff.

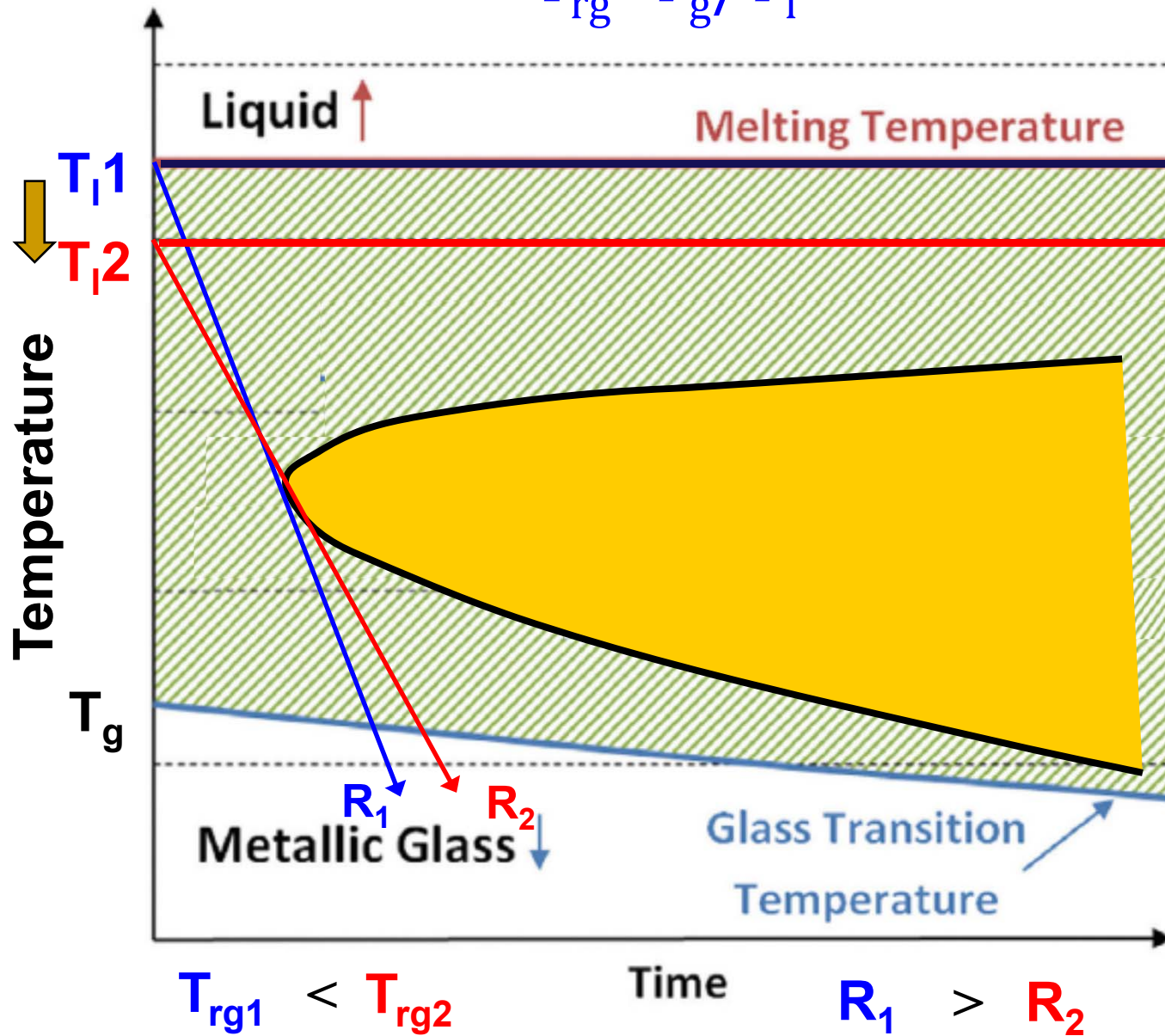
Time Temperature Transformation diagram:

$$T_{rg} = T_g / T_l$$



Time Temperature Transformation diagram:

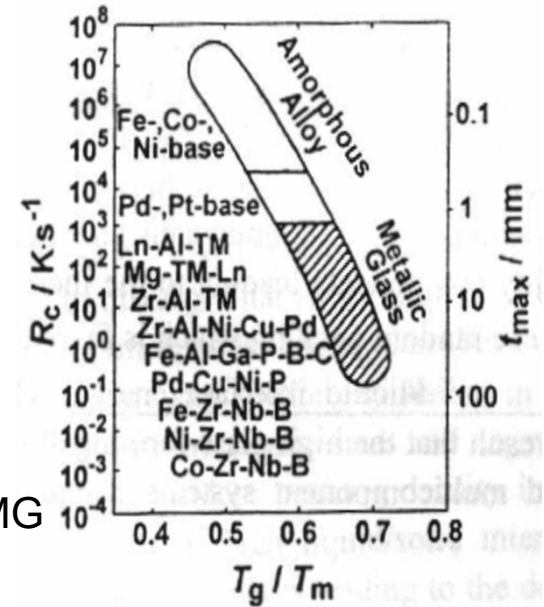
$$T_{rg} = T_g / T_l$$



GFA Parameters on the basis of thermodynamic or kinetic aspects :

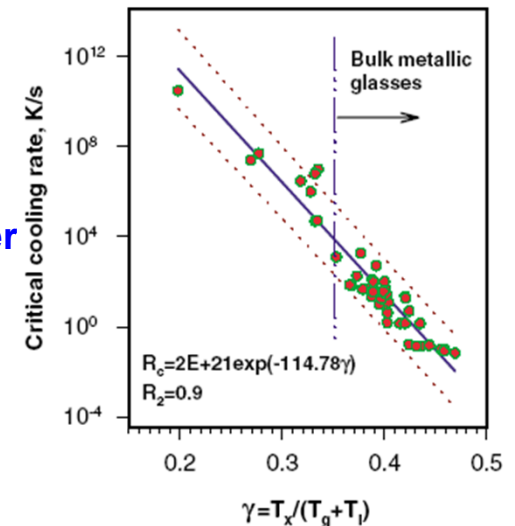
4) T_{rg} parameter = T_g/T_l

- kinetic approach to avoid crystallization before glass formation
- Viscosity at T_g being constant, the higher the ratio T_g/T_l , the higher will be the viscosity at the nose of the CCT curves, and hence the smaller R_c
- $T_l \downarrow$ and $T_g \uparrow \blacktriangleright$ lower nucleation and growth rate \blacktriangleright GFA \uparrow
 - significant difference between T_l and T_g in multi-component BMG
 - insufficient information on temperature-viscosity relationship
 - insufficient correlation with GFA



5) γ parameter = $T_x / (T_l + T_g)$

- thermodynamic and kinetic view points - **relatively reliable parameter**
- stability of equilibrium and metastable liquids: T_l and T_g
- resistance to crystallization: T_x



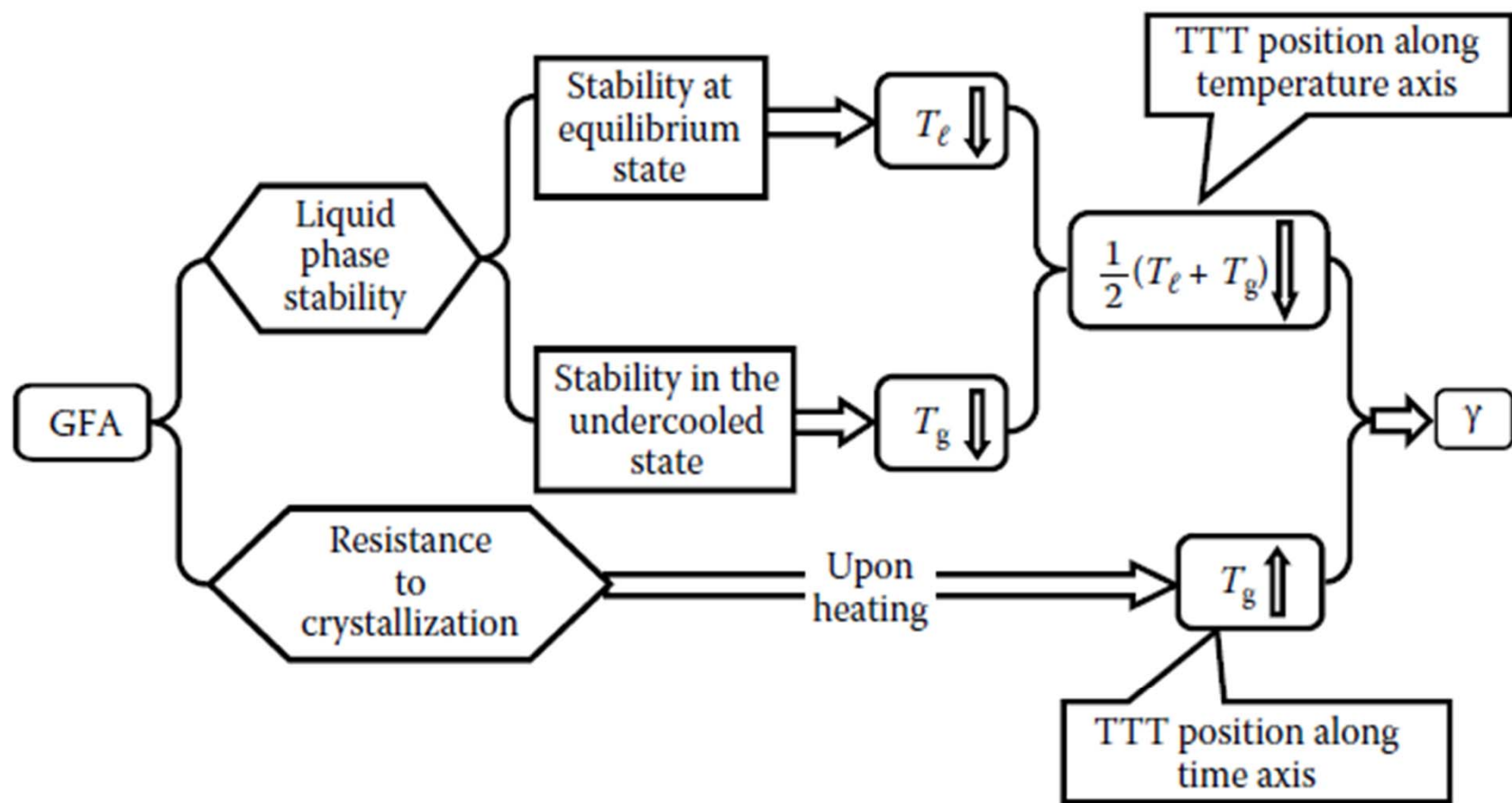
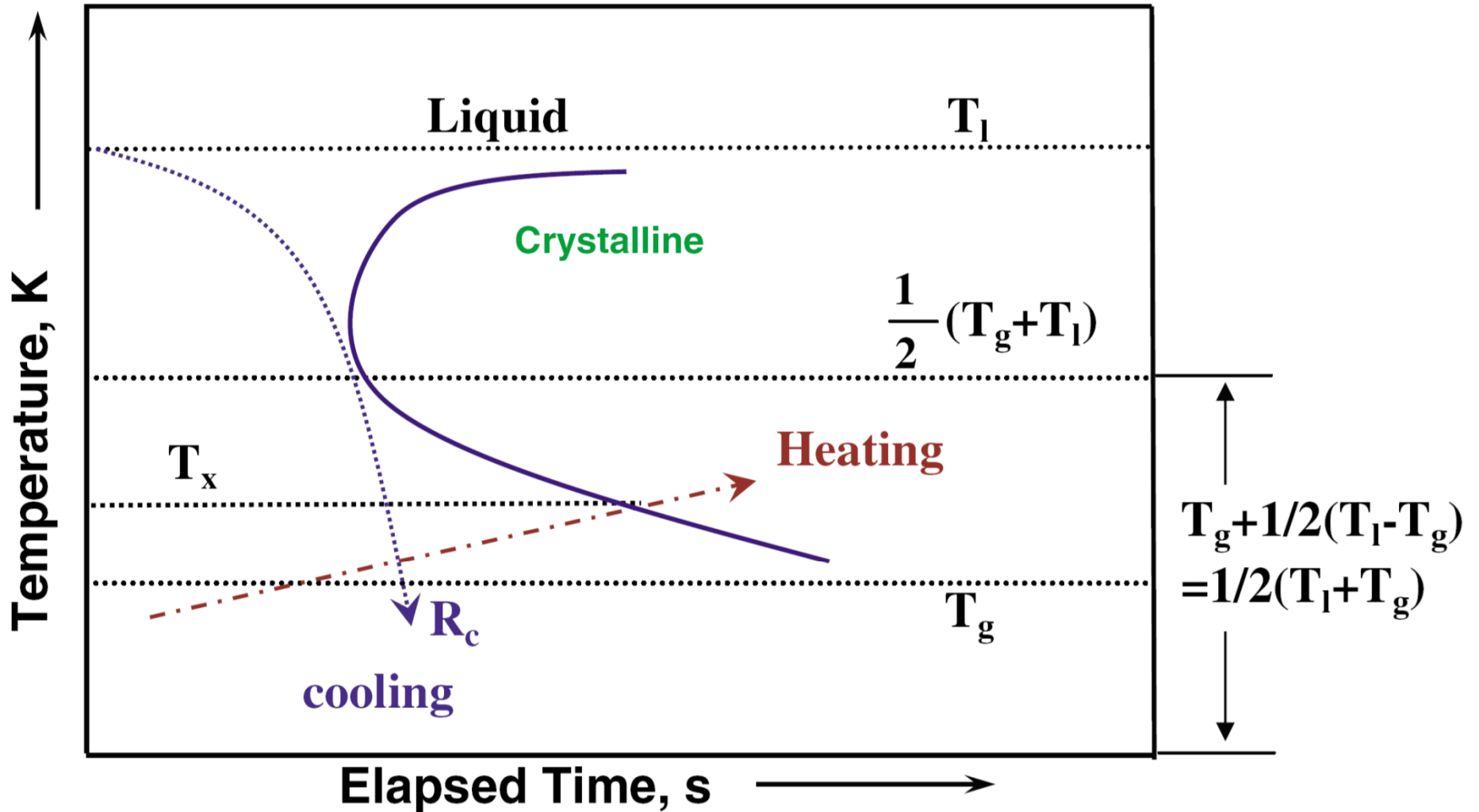


FIGURE 3.8

Schematic to illustrate the different factors involved in deriving the γ parameter to explain the GFA of alloys. (Reprinted from Lu, Z.P. and Liu, C.T., *Intermetallics*, 12, 1035, 2004. With permission.)

$$\gamma \propto T_x \left[\frac{1}{2(T_g + T_1)} \right] \propto \frac{T_x}{T_g + T_1}$$



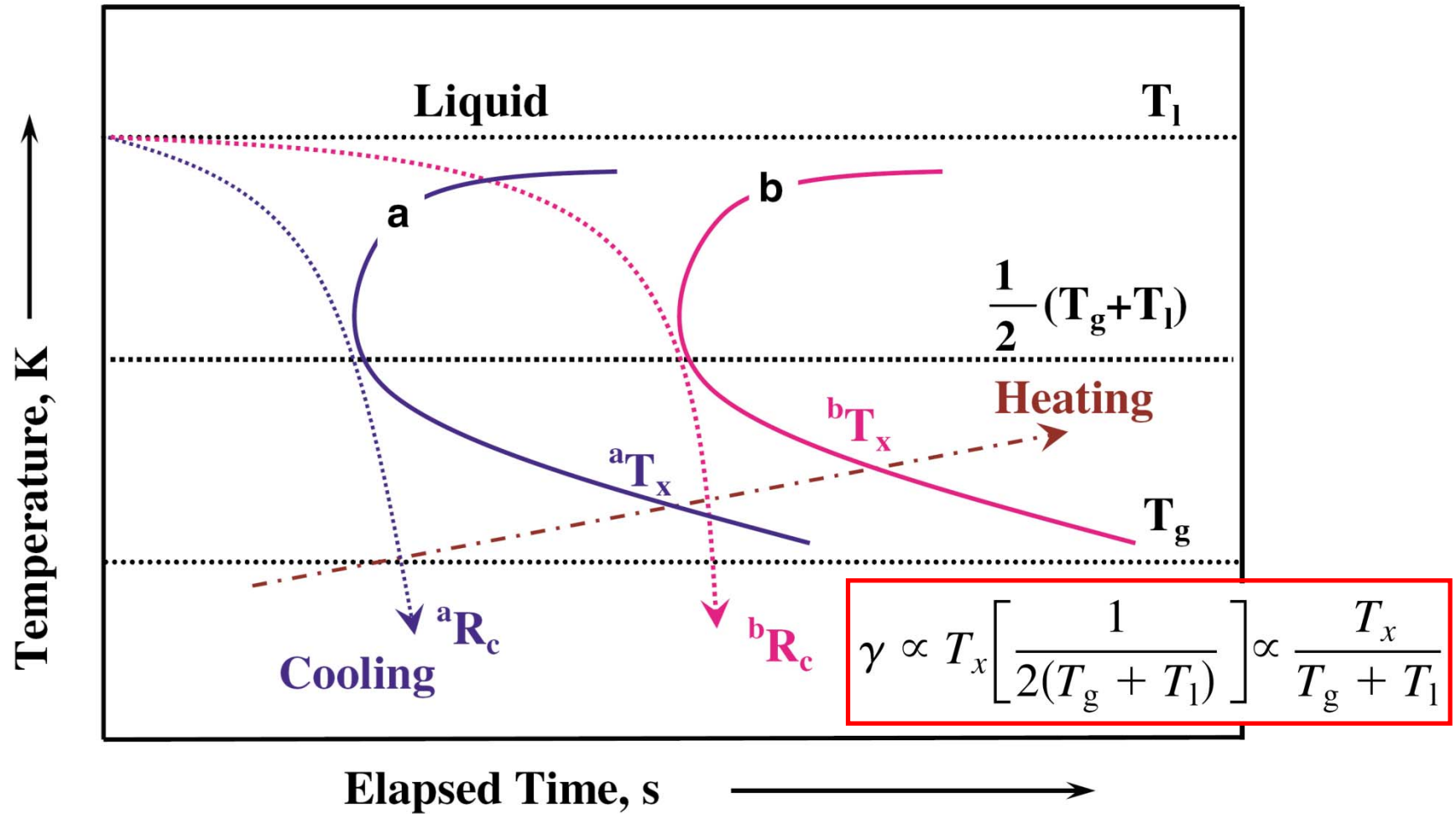


FIG. 2 (color online). Schematic TTT curves showing the effect of T_x measured upon continuous heating for different liquids with similar T_1 and T_g ; liquid b with higher onset crystallization temperature bT_x (${}^aT_x < {}^bT_x$) shows a lower critical cooling rate bR_c (${}^bR_c < {}^aR_c$).

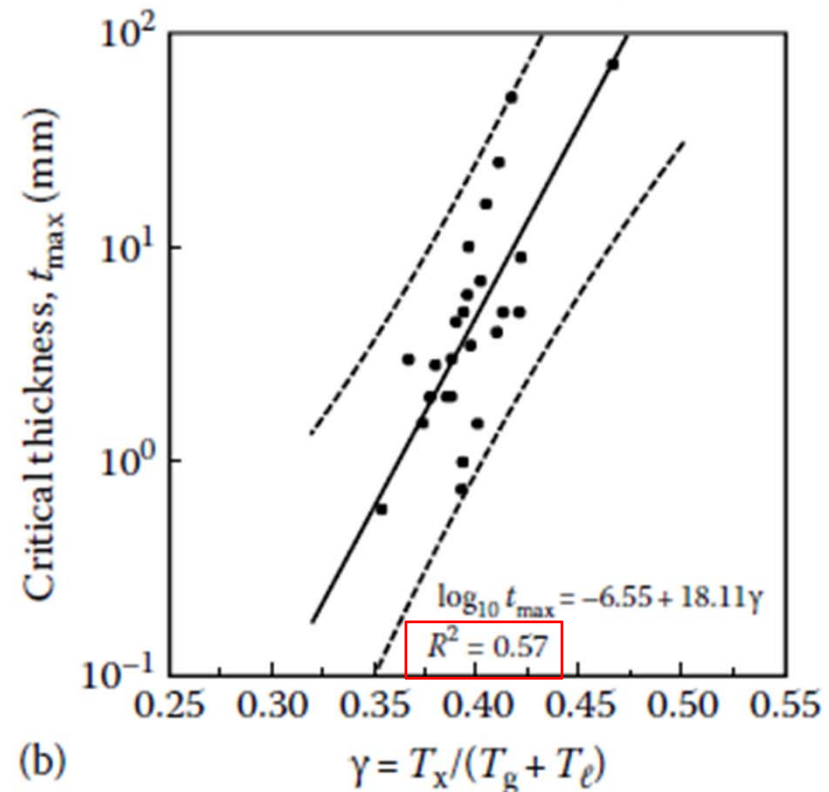
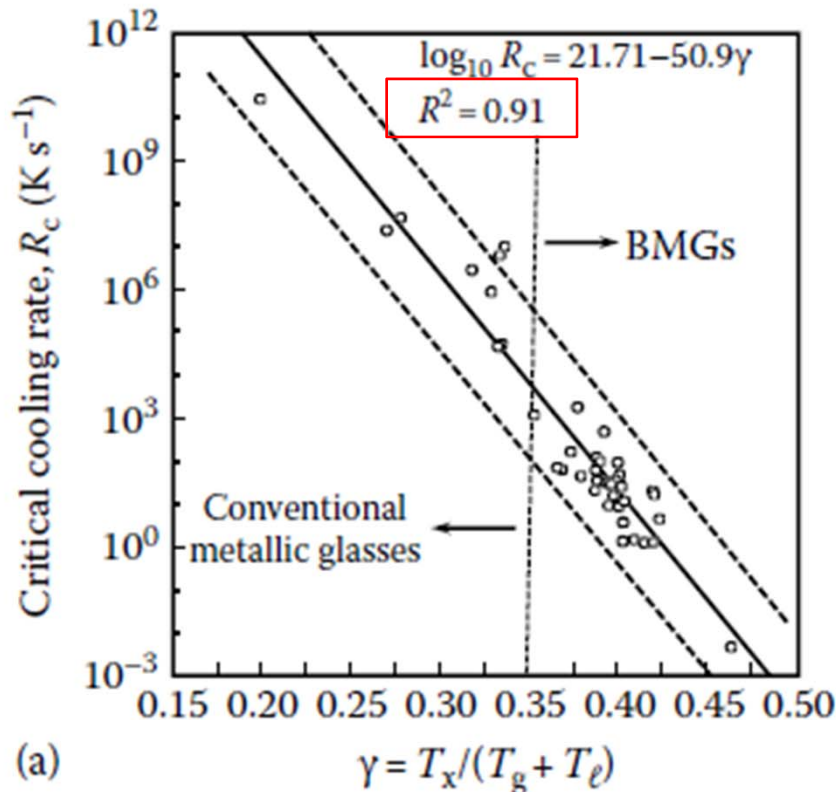
$$\log_{10} R_c = (21.71 \pm 1.97) - (50.90 \pm 0.71) \gamma \quad \log_{10} t_{\max} = (-6.55 \pm 1.07) + (18.11 \pm 0.70) \gamma$$

$$R_c = R_0 \exp\left[\left(-\frac{\ln R_0}{\gamma_0}\right) \gamma\right]$$

$$t_{\max} = t_0 \exp\left[\left(-\frac{\ln t_0}{\gamma_1}\right) \gamma\right]$$

$$R_c = 5.1 \times 10^{21} \exp(-117.2\gamma)$$

$$t_{\max} = 2.80 \times 10^{-7} \exp(41.7\gamma)$$



Wide scatter for the t_{\max} correlation

FIGURE 3.9

(a) Correlation between the critical cooling rate (R_c) and the γ parameter for BMGs. (b) Correlation between the maximum section thickness (t_{\max}) and the γ parameter for BMGs. (Reprinted from Lu, Z.P. and Liu, C.T., *Acta Mater.*, 50, 3501, 2002. With permission.)

GFA Parameters *on the basis of thermodynamic or kinetic aspects*

GFA parameters	Expression	Year established
T_{rg}	T_g / T_l	1969 D.Turnbull,Contemp.Phys.10(1969) 473
K	$(T_x - T_g) / (T_l - T_x)$	1972 A.Hruby, Czech. J.Phys. B 22 (1972) 1187
ΔT^*	$(T_m^{mix} - T_l) / T_m^{mix}$	1978 I.W.Donald, J.Non-Cryst.Solids 30 (1978) 77
ΔT_x	$T_x - T_g$	1993 A.Inoue, J.Non-Cryst.Solids 156-158(1993)473
γ	$T_x / (T_l + T_g)$	2002 Z.P.Lu, C.T.Liu, Acta Mater. 50 (2002) 3501
δ	$T_x / (T_l - T_g)$	2005 Q.J.Chen,Chiness Phys.Lett.22 (2005) 1736
α	T_x / T_l	2005 K.Mondal, J.Non-Cryst.Solids 351(2005) 1366
β	$T_x / T_g + T_g / T_l$	2005 K.Mondal, J.Non-Cryst.Solids 351(2005) 1366
φ	$(T_g / T_l)(T_x - T_g / T_g)^a$	2007 G.J.Fan,J.Non-Cryst. Solids 353 (2007) 102
γ_m	$(2T_x - T_g) / T_l$	2007 X.H.Du,J.Appl.phys.101 (2007) 086108
β	$(T_g / T_l - T_g)(T_g / T_l - T_g)$	2008 Z.Z.Yuan, J. Alloys Compd.459 (2008)
ξ	$\Delta T_x / T_x + T_g / T_l$	2008 X.H.Du,Chinese Phys.B 17(2008) 249